

Geology of the Continental Margin beneath Santa Monica Bay, Southern California, from Seismic-Reflection Data

by Michael A. Fisher, William R. Normark, Robert G. Bohannon,
Ray W. Sliter, and Andrew J. Calvert

Abstract We interpret seismic-reflection data, which were collected in Santa Monica Bay using a 70-in³ generator-injector air gun, to show the geologic structure of the continental shelf and slope and of the deep-water, Santa Monica and San Pedro Basins. The goal of this research is to investigate the earthquake hazard posed to urban areas by offshore faults. These data reveal that northwest of the Palos Verdes Peninsula, the Palos Verdes Fault neither offsets the seafloor nor cuts through an undeformed sediment apron that postdates the last sea level rise. Other evidence indicates that this fault extends northwest beneath the shelf in the deep subsurface. However, other major faults in the study area, such as the Dume and San Pedro Basin Faults, were active recently, as indicated by an arched seafloor and offset shallow sediment. Rocks under the lower continental slope are deformed to differing degrees on opposite sides of Santa Monica Canyon. Northwest of this canyon, the continental slope is underlain by a little-deformed sediment apron; the main structures that deform this apron are two lower-slope anticlines that extend toward Point Dume and are cored by faults showing reverse or thrust separation. Southeast of Santa Monica Canyon, lower-slope rocks are deformed by a complex arrangement of strike-slip, normal, and reverse faults. The San Pedro Escarpment rises abruptly along the southeast side of Santa Monica Canyon. Reverse faults and folds underpinning this escarpment steepen progressively southeastward. Locally they form flower structures and cut downward into basement rocks. These faults merge downward with the San Pedro Basin fault zone, which is nearly vertical and strike slip. The escarpment and its attendant structures diverge from this strike-slip fault zone and extend for 60 km along the margin, separating the continental shelf from the deep-water basins. The deep-water Santa Monica Basin has large extent but is filled with only a thin (less than 1.5-km) section of what are probably post-Miocene rocks and sediment. Extrapolating ages obtained from Ocean Drilling Program site 1015 indicates that this sedimentary cover is Quaternary, possibly no older than 600 ka. Folds and faults along the base of the San Pedro Escarpment began to form during 8–13 ka ago. Refraction-velocity data show that high-velocity rocks, probably the Catalina Schist or Miocene volcanic rocks, underlie the sedimentary section. The San Pedro Basin developed along a strike-slip fault, widens to the southeast, and is deformed by faults having apparent reverse separation and by folds near Redondo Canyon and the Palos Verdes Peninsula.

Introduction

The high population density and active tectonics of the urban Los Angeles region combine to heighten the risk of significant loss from major earthquakes. Recent quakes, notably those at Whittier Narrows (1987, M_L 5.9) and at Northridge (1994, M_w 6.7), underscored the hazard and the economic threat posed by the numerous faults known to crosscut this region. Of late, much research has focused on the lo-

cation and displacement history of onshore faults (e.g., Legg, 1987; Greene and Kennedy, 1987; Shaw and Suppe, 1996; Shaw and Shearer, 1999; Dolan *et al.*, 2000; Weaver and Dolan, 2000; Tsutsumi *et al.*, 2001). Offshore faults, however, are difficult and expensive to study, so in general, our understanding of them lags greatly. Even so, compilations of southern California seismicity (e.g., Hauksson and Sal-

vidar, 1989; Ziony and Jones, 1989; Goter, 1992; Jennings, 1994; Petersen and Wesnousky, 1994) show that offshore earthquakes can have at least moderate magnitude. Two earthquakes named after the coastal town of Malibu occurred in 1979 (M_L 5.2) and 1989 (M_L 5.0), about 12 km beneath Santa Monica Bay, west of Los Angeles (Fig. 1). The largest earthquake known to have struck the coastal area was the 1933 Long Beach event (M_L 6.4), which occurred along the

Newport–Inglewood strike-slip fault. These earthquakes provide some impetus to better understand the hazard posed by offshore faults.

In this report we use marine seismic-reflection data to investigate the offshore geologic structure with the ultimate goals of locating active faults and estimating their displacement histories. Toward these goals, during the years 1998–2000 the U.S. Geological Survey conducted three marine

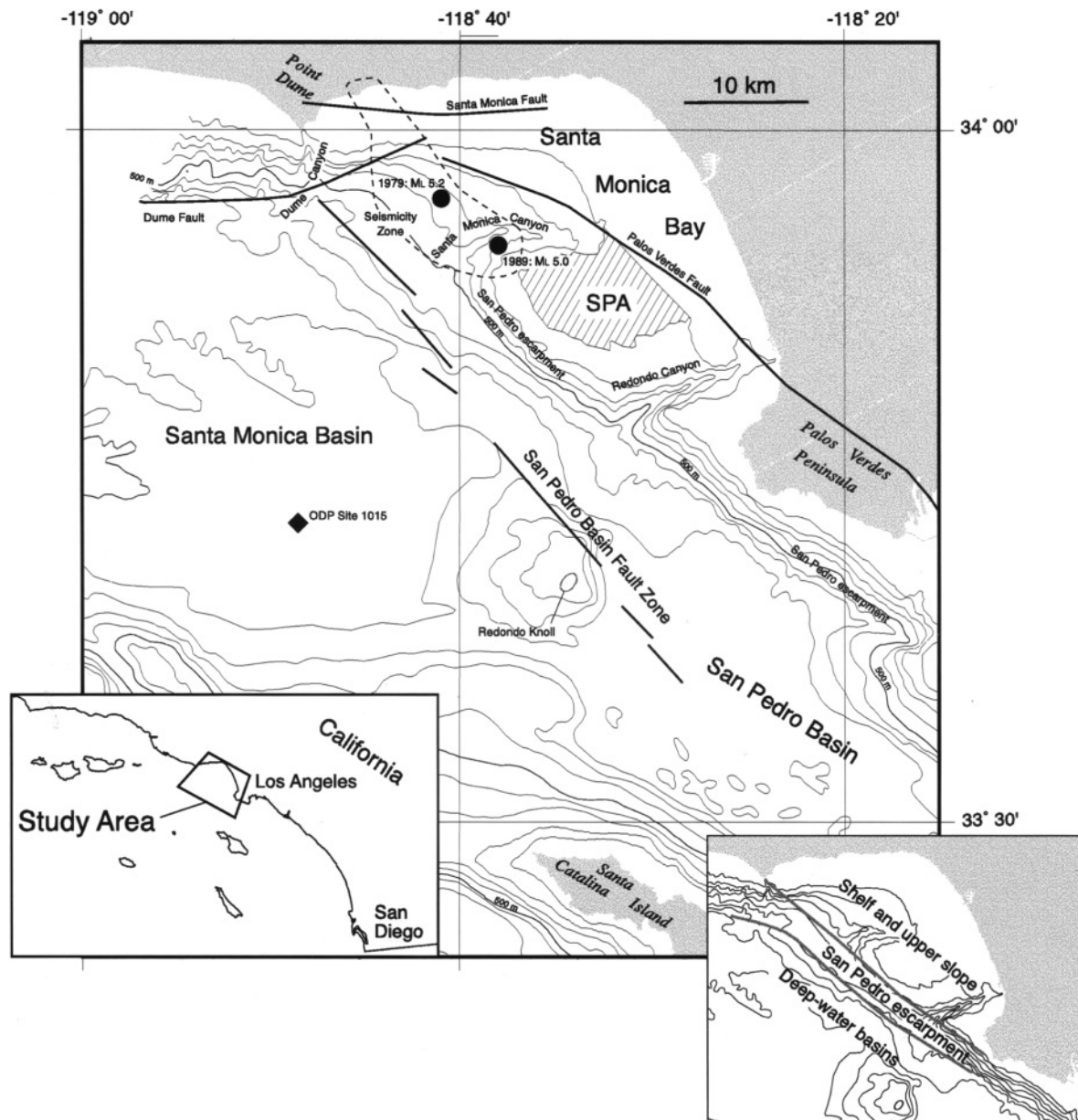


Figure 1. Index map of the study area, showing the main geographic features, the zone of active seismicity under northwestern Santa Monica Bay (dashed outline), epicenters of the Malibu earthquakes, and offshore faults. The cross-hatched area labeled “SPA” shows where sedimentary rocks below shallow flat-lying sediment are folded tightly, making up the shelf projection anticlinorium. Faults adapted from Junger and Wagner (1977), Greene and Kennedy (1987), Wright (1991), and Dolan *et al.* (2000). The left inset figure shows the regional location of the study area. The right inset figure shows how the study area is divided into three belts for discussion.

seismic surveys to collect high- and medium-resolution, seismic-reflection data along parts of the coast between Los Angeles and San Diego. These surveys are a preamble to a more complete effort to study offshore faults, which involves merging findings from seismic-reflection data with age dates from sediment collected during coring operations to characterize shallow deformation along the continental shelf and upper slope.

The study area for this report encompasses the continental shelf under Santa Monica Bay as well as the eastern part of the deep-water Santa Monica and San Pedro Basins to the southwest (Fig. 1). This area is bounded on the north by the Santa Monica Mountains and the active Santa Monica, Dume, and Malibu Coast Faults; on the east by the deep and petroliferous Los Angeles Basin; and on the southeast by the active structural culmination that underlies the Palos Verdes Peninsula.

Geophysical Data

In this report, we use a variety of marine seismic-reflection data to decipher the offshore structure. We rely primarily on medium-resolution, multichannel seismic (MCS) data that were obtained using a 70-in³ air gun, but also we use high-resolution seismic data collected with small electrical sources. Sparse, deep-crustal seismic-reflection data provide local windows into deep rocks, a complex realm that the lower-powered seismic-reflection systems were unable to penetrate.

Small-air-gun, MCS reflection data were collected during three cruises. Detailed operational reports for the cruises are available online (Normark *et al.*, 1999a,b; Gutmacher *et al.*, 2000). The main MCS streamer was 240 m long and had 24 channels, with 10-m groups and three hydrophones per group. The primary sound source was a dual-chambered (both 35 in³), generator-injector air gun. In operation, the second chamber fires about 15 msec after the first to minimize bubble oscillations. This air gun was suspended from a float to maintain a constant depth of 1 m, and it was fired every 12 sec with an air pressure of 3000 psi. A backup seismic-reflection system, only occasionally used, included a streamer that was 100 m long and had 24 channels with 6.25-m groups and one phone per group. The alternate sound source was a 40-in³ Bolt air gun, with a wave-shape kit to reduce bubble oscillations, which was towed at a depth of about 4 m and fired every 6 sec. The nominal air pressure was 2000 psi. All seismic-reflection data are 24-fold and were migrated after stack. Tracklines for data used in this report are shown in Figure 2.

Some high-resolution seismic reflection data were collected with a Huntec deep tow system, which is a boomer on a platform that is towed between 6 and 160 m below the sea surface, depending upon the overall water depth. This seismic system was used to image the upper few tens of milliseconds of strata with a resolution of better than 0.5 msec (<0.4 m assuming water acoustic velocity). The

frequency spectrum of the emitted sound peaks between 1.5 and 5 kHz. A surface-towed, Geopulse boomer system was used in the shallow-water, particularly the inshore, parts of the survey area, in water depths from 20 to 300 m. The sound source consists of two Geopulse boomer plates mounted on a catamaran. The effective bandwidth of the Geopulse system is about 750–3500 Hz.

Before each of the three annual surveys, permits had to be obtained to operate seismic sources near the abundant marine-mammal populations off southern California. This approval entailed gaining separate permits from each of the National Marine Fisheries Service, the California Coastal Commission, and the California State Lands Commission. An online report describes the procedures followed (Childs *et al.*, 1999). These permits constrained three aspects of the seismic survey: (1) the size of the acoustic source (it had to be small, less than about 100 in³), (2) where the source could be used (e.g., farther than 3 miles from shore), and (3) when it could be used (e.g., only during daylight). The prohibition against inshore surveys meant that we could investigate only with low-powered seismic systems some active faults that are of particular concern because of their proximity to urban areas. The restriction to small sound sources greatly limited the maximum depth from which we obtained information, so earthquake source regions that are deeper than about 2 km in the Earth cannot be studied or mapped. We lost much survey time because of the restriction to daylight-only operations, with the result that seismic-reflection data were obtained along only a few of the planned east–west cross lines in the seismic grid (Fig. 2).

In 1994, deep-crustal seismic-reflection data were collected off southern California for the Los Angeles Regional Seismic Experiment (LARSE) (Brocher *et al.*, 1995) (tracklines shown in Fig. 2). These data were the last to be collected by academia off California with a powerful air-gun array before the imposition of strict regulations designed to protect marine mammals. These 40-fold data were collected aboard the R/V *Maurice Ewing* using a source array of 20 air guns with a total chamber volume of 137.7 L (8470 in³). The digital streamer was 4200 m long and had 160 data channels. Previous reports show data from the LARSE experiment (ten Brink *et al.*, 2000; Fuis *et al.*, 2001).

We present tomographic refraction velocities, from an area of the continental shelf that was determined from data collected along the MCS streamer during the LARSE experiment. When calculating these velocities, we edited seismic data to remove low-quality recording channels and bad shots, and the first arrivals were picked for every shot to within 8 msec. First-arrival travel times for direct, sub-seafloor-turning, and diffracted waves numbered nearly 167,000, and all were input to an iterative, two-dimensional tomographic inversion algorithm that is based on a finite-difference solution to the eikonal equation (Aldridge and Oldenburg, 1993). The vertical and horizontal spacing of the grid of velocity values was 12.5 m.

Other public-domain, MCS data were obtained by the

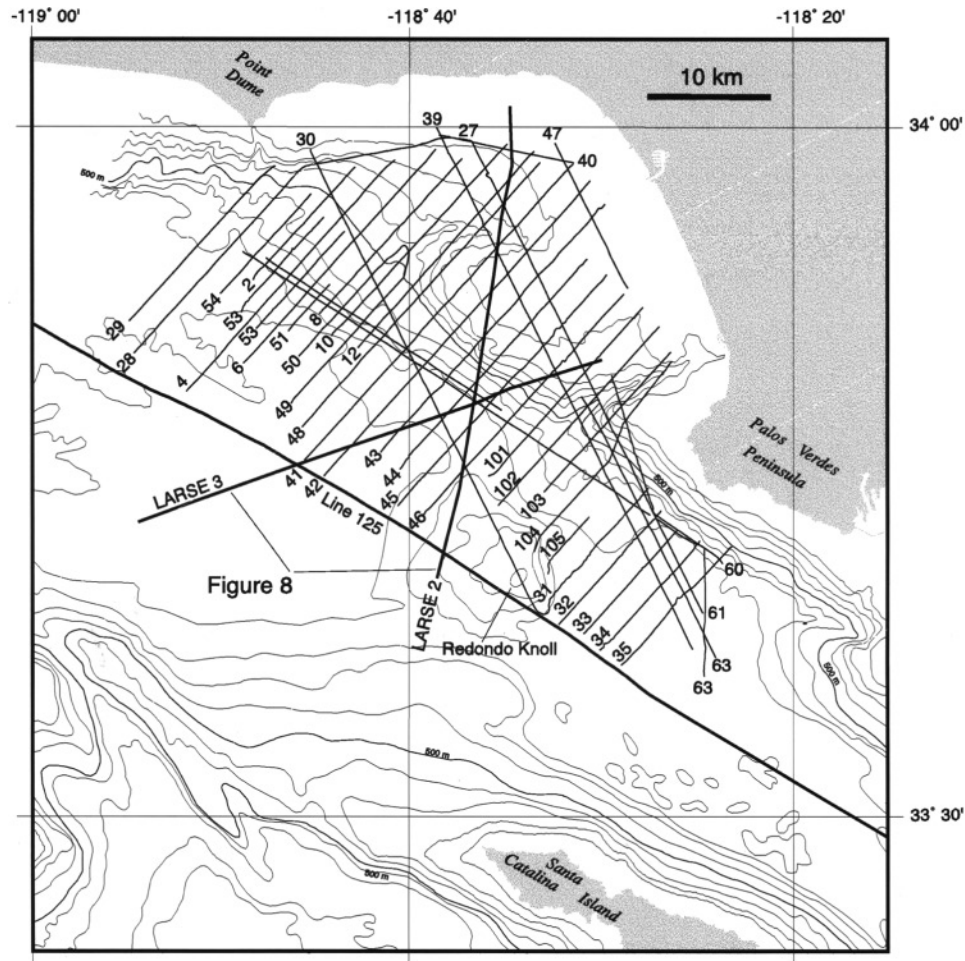


Figure 2. Grid of small-air-gun multichannel seismic (MCS) data (lightweight lines), the main basis for this report, and locations of large-air-gun MCS data collected during the LARSE (lines 2 and 3) and U.S. Geological Survey (line 125) surveys. See text for distinction between small- and large-air-gun data.

U.S. Geological Survey in 1990 (Bohannon *et al.*, 1990). These data are critical to study of the regional geologic framework, and some of these data have been described and interpreted elsewhere (Bohannon and Geist, 1998). Seismic line 125 from this survey transits the deep-water part of our study area (Fig. 2). These data are 22-fold and were collected with a 39.7 L (2424 in³) air-gun array and a 2600-m-long streamer.

Offshore Stratigraphy and Structure

Early and Middle Miocene Geology

The California Continental Borderland developed during two main phases of late Cenozoic deformation (e.g., Vedder, 1987; Wright, 1991; Crouch and Suppe, 1993; Bohannon and Geist, 1998; ten Brink *et al.*, 2000). The older phase, spanning early and middle Miocene time, involved regional, oblique extension of the borderland region. The second, middle Pliocene and more recent phase involved the

north part of the borderland in transpressive deformation. This two-phase deformation produced a complex distribution of compressive, strike-slip, and extensional structures.

Paleomagnetic data have been interpreted to suggest that early and middle Miocene extension occurred in conjunction with the clockwise, vertical-axis rotation of the western Transverse Ranges (Kamerling and Luyendyk, 1979; Luyendyk *et al.*, 1980, 1985; Hornafius *et al.*, 1986). The main geologic structures within these mountains strike west, in contrast to the northwest strike of major geologic structures south of the mountains, within this report's offshore study area. The crust within the study area was greatly attenuated during extension, in the wake of the rotating western Transverse Ranges. Extension progressed to the point that blueschist and amphibolite facies metamorphic rocks, assigned to the Catalina Schist, made up the footwall of the detachment and were uplifted from great depth and exposed at the surface. Evidence from drilling offshore and within the Los Angeles Basin and seismic-reflection data indicate that the Catalina Schist occurs within a wide belt below the

inner part of the borderland, where it directly underlies Miocene and younger, sedimentary, volcanoclastic and volcanic rocks. This schist constitutes the basement complex beneath the study area (e.g., Vedder, 1987; Wright, 1991; Bohannon and Geist, 1998; ten Brink *et al.*, 2000).

Widespread volcanism associated with the crustal extension commenced during the early Miocene and culminated during the middle Miocene (Weigand *et al.*, 1998). Rapid uplift and erosion resulted in clasts of Catalina Schist being deposited in the Miocene San Onofre breccia (Stuart, 1979). As the heat-flow anomaly caused by the crustal extension dissipated, the region subsided. The volcanic rocks and breccia are succeeded stratigraphically by widespread, middle and late Miocene chert and shale that make up the Monterey Formation (e.g., Woodring *et al.*, 1946; Barron and Isaacs, 2001).

Early Pliocene and Quaternary Geology

The present, transpressional tectonic regime of the Southern California Borderland dates back to the early or middle Pliocene, about 6 Ma ago (Atwater, 1970, 1998; Wright, 1991; Crouch and Suppe, 1993). The transition from extension to transpression, of fundamental importance to the development of the northern part of the borderland, was caused by a shift in plate-boundary motion from offshore eastward to the southern San Andreas Fault. This transition in stress regime activated pre-existing, favorably oriented structures so that a northwest–southeast, compressional and strike-slip structural grain developed within margin rocks (Wright, 1991; Dolan *et al.*, 1995; Shaw and Suppe, 1996; Schneider *et al.*, 1996; Walls *et al.*, 1998; Shaw and Shearer, 1999). A possible consequence of the shift in direction of regional compression is that some middle Miocene extensional faults were reactivated as thrust and strike-slip faults. Also blind thrust faults and fault-propagation folds may have formed beneath the densely populated Los Angeles region to constitute one of the chief earthquake threats (e.g., Davis *et al.*, 1989; Davis and Namson, 1994a,b; Shaw and Suppe, 1996).

The north boundary of the study area lies along the Santa Monica, Dume, and Malibu Coast Faults as well as the deep and blind Santa Monica Mountains thrust fault (Fig. 1). These faults and structures share the west strike of the western Transverse Ranges. Collectively these faults border the offshore area where the Catalina Schist belt is at relatively shallow depth beneath Neogene rocks. The blind, Santa Monica Mountains thrust fault (originally called the Elysian Park thrust [Davis and Namson, 1994a]) is interpreted to lie at depth below the Malibu Coastal and Dume Faults (Davis *et al.*, 1989; Davis and Namson, 1994a,b; Dolan *et al.*, 1995; Sorlien, 1999; Dolan *et al.*, 2000). This blind thrust fault probably developed originally as an extensional detachment that accommodated the Miocene, clockwise rotation of the western Transverse Ranges (Crouch and Suppe, 1993; Dolan *et al.*, 1995; Sorlien, 1999). During the Miocene extension, this fault appears to have been among the most

tectonically active features in the region (Crouch and Suppe, 1993; Bohannon and Geist, 1998).

Northeast of the study area near the city of Los Angeles, the Santa Monica Fault strikes parallel to and crops out 3–4 km southeast of the range front of the Santa Monica Mountains (Dolan *et al.*, 2000). This fault crosses the shoreline and continues through rocks beneath northern Santa Monica Bay (Fig. 1). Dolan *et al.* (2000) summarized the offshore position of this fault from previous work based on marine seismic-reflection data. In an alternative view of offshore faulting, Junger and Wagner (1977) proposed that beneath Santa Monica Bay, the Santa Monica Fault forks into the partly onshore Malibu Coast Fault and the more southeasterly and entirely offshore Dume Fault. Both of these faults extend far to the west, to beneath the Santa Barbara Channel and through the northern Channel Islands (Sorlien, 1999).

Along the eastern boundary of the study area, the Palos Verdes Hills stand prominently above the otherwise low-lying coastal plain. The Palos Verdes Fault passes northwest of these hills, sharing the regional northwest strike of most major structures south of the Transverse Ranges (Woodring *et al.*, 1946; Yerkes *et al.*, 1965; Greene and Kennedy, 1987; Wright, 1991).

The fundamental structural style of major faults in the Los Angeles region is currently being debated. Some researchers, for example, hypothesize that only limited strike-slip offset occurs along major faults; instead the structural style is thought to be controlled by thrust or reverse movement along blind faults (e.g., Davis *et al.*, 1989; Davis and Namson, 1994a,b; Shaw and Suppe, 1996). Other geologists, however, emphasize the importance of strike- or oblique-slip offset (e.g., Nardin and Henyey, 1978; Wright, 1991; McNeilan *et al.*, 1996; Francis *et al.*, 1996; Legg *et al.*, 2001). According to this view, the main offshore geologic structures formed while convergent dextral shear occurred along the important faults; some deformation resulted from movement within restraining and releasing bends along strike-slip faults.

The Palos Verdes Fault apparently extends for more than 100 km southwestward from the northern part of Santa Monica Bay (Greene and Kennedy, 1987). This fault passes below the northwest part of the Palos Verdes Peninsula and beneath San Pedro Harbor (Woodring *et al.*, 1946; Yerkes *et al.*, 1965; Clarke *et al.*, 1983, 1985; Stephenson *et al.*, 1995; McNeilan *et al.*, 1996). Wave-cut terraces show that the peninsula has undergone rapid Quaternary and Holocene uplift. The vertical strain rate appears to be around 3 mm/yr, based on analysis of wave-cut terraces and offset stream courses (Ward and Velensie, 1994). Multibeam bathymetric data collected southeast of the Palos Verdes Peninsula have been interpreted to show the Palos Verdes Fault extending for about 60 km below the shelf, slope, and deep-water areas (Marlow *et al.*, 2000).

The geometry of the Palos Verdes Fault at depth has been variously interpreted from oil industry seismic-reflection data. For example, Davis and Namson (2002) de-

picted this fault zone with a steep southwest dip (about 60°) in the upper 5 km of the crust. Similarly, Shaw (1999) indicated that the Palos Verdes fault zone is steep to vertical in the upper 5 km of the crust, but below this depth, this fault is indicated with a dip of about 30° southwest. Shaw and Suppe (1996) tied movement along the Palos Verdes fault zone to deeper movement along the Compton thrust fault, which is proposed as a blind, northeast-dipping fault. In contrast to these interpretations that involve mainly thrust movement along the Palos Verdes Fault, Wright (1991) indicated that movement along this fault is mainly strike slip, and this fault is vertical or steeply east dipping (Junger and Wagner, 1977; Nardin and Henyey, 1978), at least for depths shallower than about 9 km.

Nardin and Henyey (1978) proposed that deformation of strata below the coast and outer shelf is concentrated in five main zones that they referred to as anticlinoria. The shelf projection anticlinorium (cross-hatched area labeled "SPA" in Fig. 1) deforms rocks south of Santa Monica Canyon. Formation of anticlinoria is attributed to convergent dextral shear along the Palos Verdes Fault.

Present Setting

The shallow Santa Monica shelf and adjacent continental slope are deeply incised by three submarine canyons, which are, from northwest to southeast, the Dume, Santa Monica, and Redondo Canyons (Fig. 1). Underlying geologic structures may control the courses these canyons follow; some authors, for example, have suggested that Redondo Canyon marks the location of Redondo Canyon thrust fault (Nardin and Henyey, 1978; Wright, 1991).

A narrow continental shelf extends eastward from Point Dume around Santa Monica Bay to near the head of Santa Monica Canyon. In addition, a lobate area of shallow water over a nearly horizontal seafloor (SPA in Fig. 1) borders Santa Monica Canyon on the south. Complexly deformed rocks that make up the shelf projection anticlinorium (Nardin and Henyey, 1978) underlie this part of the shelf. Together these shallow areas enclose a part of the continental slope, under northeastern Santa Monica Bay, that deepens gradually southwest. The low-angle continental slope northwest of Santa Monica Canyon gives way abruptly across the canyon to the San Pedro Escarpment, and farther southeast lie the high-relief Palos Verdes Hills (Fig. 1). The escarpment is a relatively steep section of the continental margin, having an average slope of about 10°. The escarpment continues to the southeast, outside the study area.

Seismic-reflection and wide-angle-seismic data indicate that under Santa Monica Bay, a subsurface basement ridge made up of Catalina Schist extends northwest-southeast beneath the continental shelf and slope (Wright, 1991; ten Brink *et al.*, 2000). This ridge is a fundamental feature of the offshore area because it separates the onshore Los Angeles sedimentary basin from deep-water basins of the California Continental Borderland. Thin (0.5–1 km) Neogene and Quaternary sedimentary rocks cover the basement ridge

(Wright, 1991). On seismic sections these rocks appear to thicken sharply off crest, northeastward into the Los Angeles Basin and southwestward in the deep-water Santa Monica and San Pedro Basins. Under the continental shelf within the study area, the contact between sedimentary rocks and the underlying Catalina Schist forms the acoustic basement in our seismic-reflection data (e.g., Vedder, 1987). Elsewhere, the acoustic basement could include the schist and Miocene volcanic rocks and breccia.

Drilling at Ocean Drilling Program (ODP) site 1015, located in the southwestern Santa Monica Basin (Fig. 1), where the sediment cover over metamorphic basement is thin, provides the main age constraint on sedimentary rocks within the deep-water Santa Monica Basin. The drill penetrated Quaternary turbidites at 150 m depth that are no older than 60 ka (Shipboard Scientific Party, 1997; Normark *et al.*, 1998). The deep-water San Pedro and Santa Monica Basins are separated from each other by the Redondo Knoll (Fig. 1), which is underlain by Miocene volcanic and volcanoclastic rocks that are covered by a veneer of sediment (Vedder, 1990). In the San Pedro Basin, rocks of post-Miocene age are thickest (about 2 km) southwest of the Palos Verdes Peninsula (Vedder, 1987; Teng and Gorsline, 1989). Such rocks in the Santa Monica Basin are about 2.5 km thick west of the study area, between Point Dume and Santa Cruz Island. Within the study area, post-Miocene basin rocks are only about 1 km thick.

An Offshore Seismic Zone

Within the area encompassed by Figure 1, the two largest offshore earthquakes, the Malibu events ($\sim M_L 5$), fall within a cluster of smaller-magnitude earthquakes that stretches from the northwest end of the San Pedro Escarpment northwestward to near Point Dume (dashed outline in Fig. 1) (Hauksson and Saldívar, 1986, 1989). The Malibu earthquakes nucleated at a depth of about 10 km, so this seismicity does not correlate directly with the shallow faults and folds that are evident in seismic reflection data shown here. Even so, such structures might provide clues to help understand deeper structures that do control earthquake distribution, in particular the extent and continuity of deep features.

Observations from MCS Data

Structure under the Continental Shelf and Upper Slope

For the sake of discussion, we subdivide the continental margin under and west of Santa Monica Bay into three, southeast-trending belts (see map inset on lower right of Fig. 1; the main structures in each belt are shown in Fig. 3). The first belt encompasses the continental shelf and upper slope that lies east of a line drawn along the San Pedro Escarpment and extended to Point Dume. The second belt consists of the San Pedro Escarpment and related northwest-trending structures that mark the juncture between the

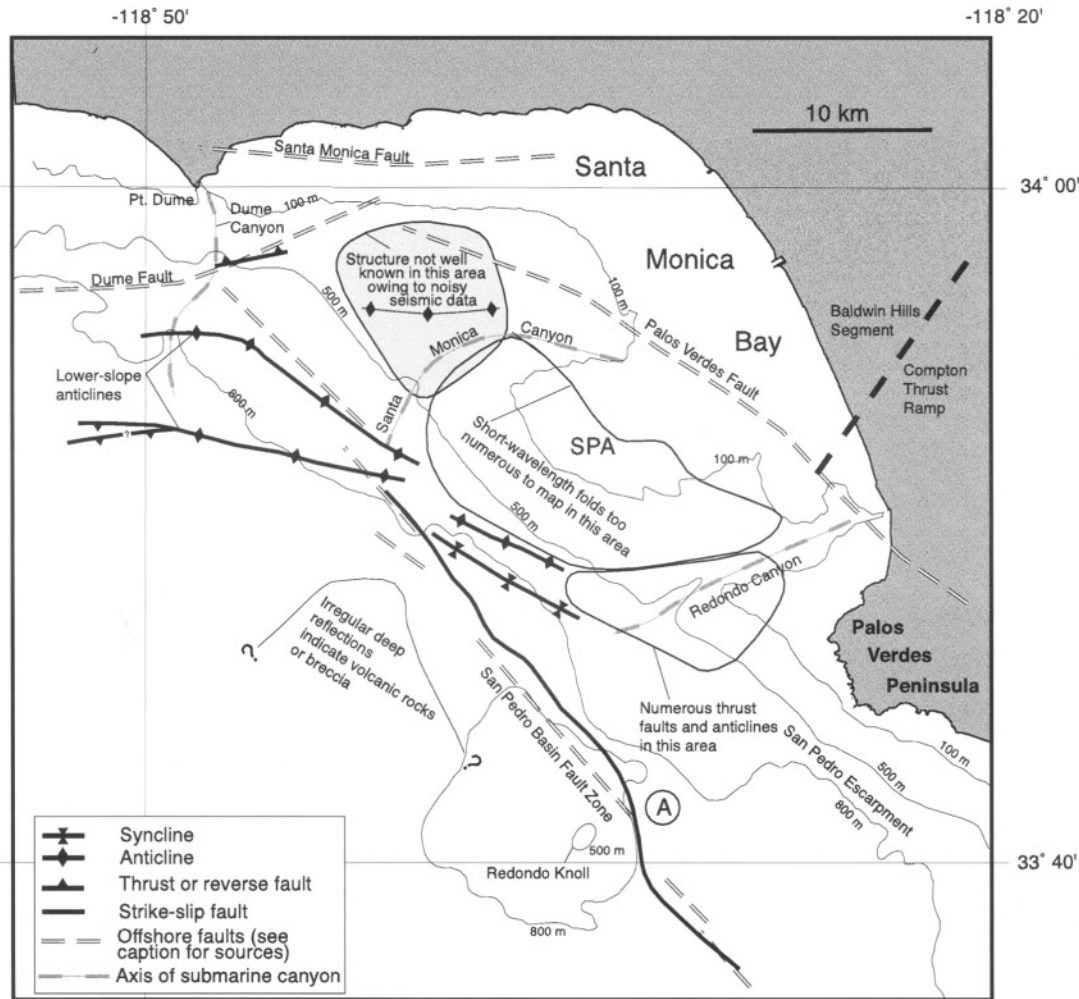


Figure 3. Main structural features interpreted from seismic-reflection data and discussed in the text. The heavy dashed line shown near the Palos Verdes Peninsula is the boundary between the most active part of the Compton thrust ramp and the less active part of the ramp, called the Baldwin Hills segment (Shaw and Suppe, 1996). Faults adapted from Junger and Wagner (1977), Greene and Kennedy (1987), Wright (1991), and Dolan *et al.* (2000). Other structures are from data in this report. SPA, shelf projection anticlinorium.

continental slope and the low-relief seafloor over the deep-water San Pedro and Santa Monica Basins. These two deep-water basins constitute the third belt.

The narrow continental shelf that rims the north side of the study area is cut by the west-striking Dume and Santa Monica Faults (Fig. 3), two major, strike-slip faults that are related to the deformation that formed the Transverse Ranges (e.g., Junger and Wagner, 1977; Wright, 1991; Dolan *et al.*, 2000). Where crossed obliquely in the offshore by seismic line 28 (Figs. 4 and 5), the Dume Fault shows reverse separation, and it deforms the overlying sedimentary section into an anticline. Unfortunately, the oblique crossing of this fault obscures the fault offset in the shallow sedimentary section. The anticline, however, deforms rocks and sediment directly under the seafloor, and the seafloor steepens over this fold (Fig. 5). At the time resolution of these

seismic-reflection data, continuous reflections from the shallow sediment section span unbroken across this fault's location.

The continental shelf under Santa Monica Bay is underlain by a basement ridge made up of Catalina Schist, and this ridge is covered by sedimentary rocks possibly as old as middle Miocene (Wright, 1991). Large-air-gun, seismic-reflection data collected along LARSE line 2 (location shown in Fig. 2) show that the upper section of these cover rocks dips and thickens northeastward toward the Santa Monica Mountains (see also ten Brink *et al.*, 2000) (Fig. 6a). The most prominent reflections near the north end of LARSE line 2 are from the base of this sedimentary section, and the reflections have an apparent dip toward the mountains (Fig. 6a).

Wide-angle velocity data from along LARSE line 2 (ten Brink *et al.*, 2000) indicate that under the continental shelf

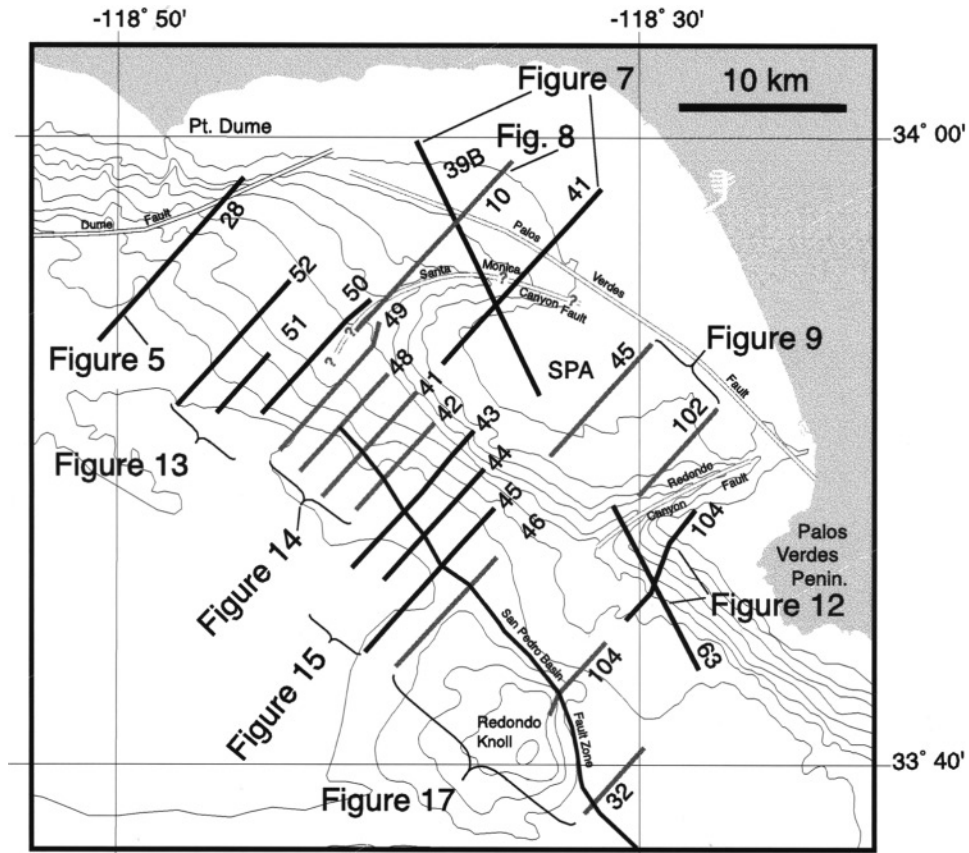


Figure 4. Locations of seismic-reflection sections shown as figures in this report. Figure 2 shows the location of large-air-gun sections in Figure 6. Black and gray lines are used to help distinguish in which figure a seismic reflection section appears. SPA, shelf projection anticlinorium.

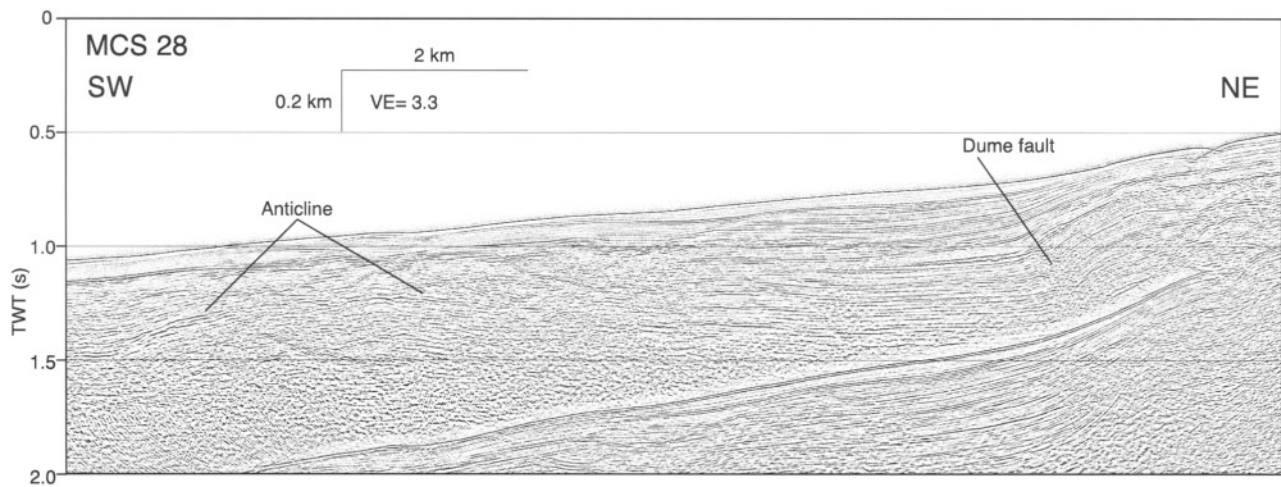


Figure 5. Poststack-migrated MCS section, location shown in Figure 4, showing the Dume Fault and one of the lower-slope anticlines. This fault arches the seafloor and shallow sediment, which attests to recent fault movement.

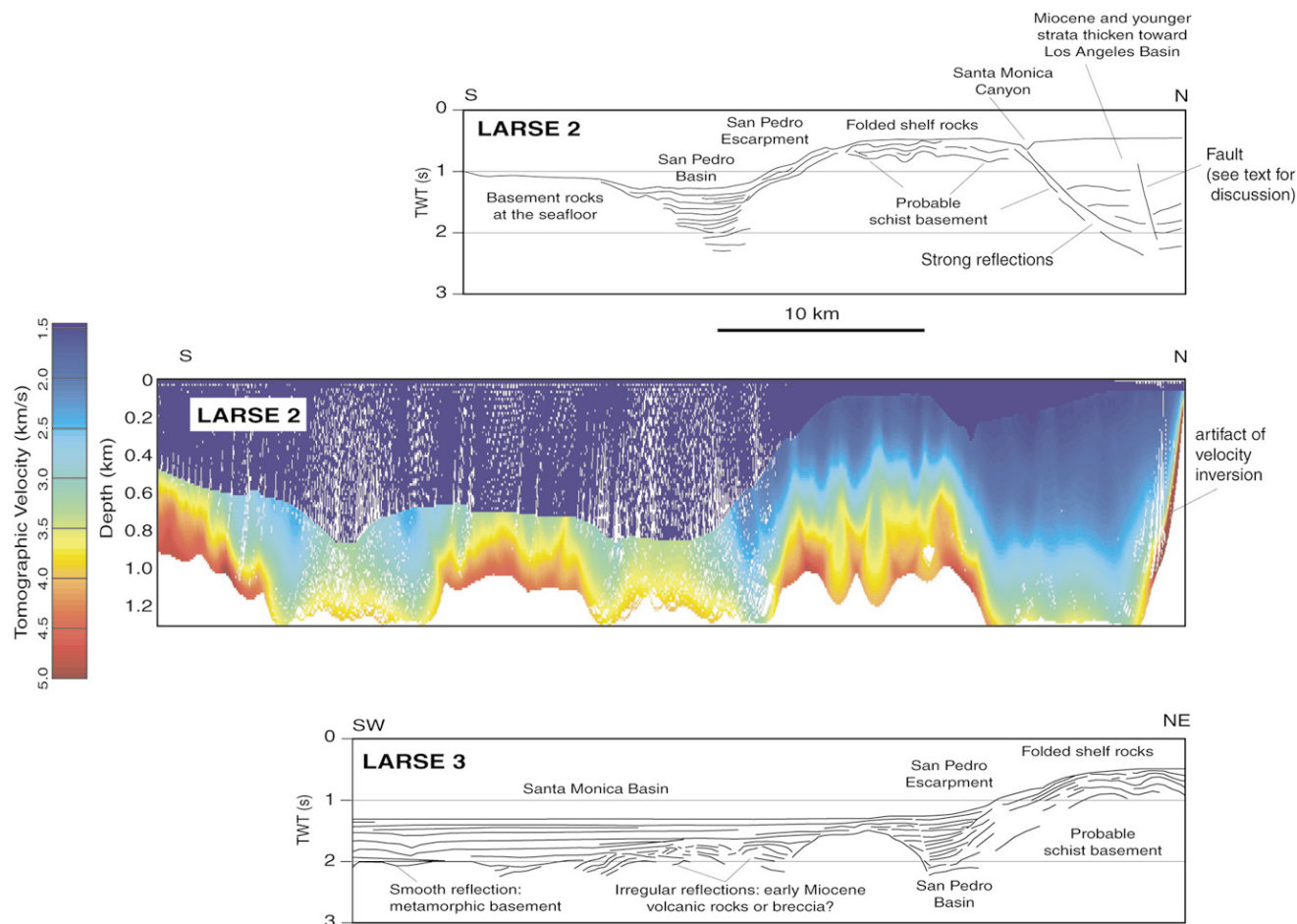


Figure 6. Line drawings of seismic-reflection data collected along LARSE lines 2 and 3. Line locations shown in Figure 2. These data show that small-air-gun data reveal the depth to volcanic rocks or metamorphic basement under the continental shelf almost as well as do the large-air-gun data. The basement contact is at shallower depth south of Santa Monica Canyon than to the north across the canyon. Tomographic velocities from section LARSE 2 show that crystalline basement is at shallow depth below the shelf.

near the north end of this line, rocks having a seismic velocity between 4 and 5 km/sec are at depths as shallow as 1 km. A similar result derives from tomographic analysis of first arrivals recorded along the seismic streamer (Fig. 6b). This analysis establishes that refraction velocities measured in rocks 900 m below the seafloor are about 4.8 km/sec. The velocities reported in ten Brink *et al.* (2000) and the accordant result shown here reveal that either volcanic rocks or schist basement rocks underlie the strongly reflective, north-dipping horizon and nearly crop out along the axis of Santa Monica Canyon. Volcanic rocks or schist is probably at shallow depth beneath the shelf area south of Santa Monica Canyon; this area includes the shelf projection anticlinorium (SPA in Fig. 1). From our velocity analysis, refraction velocities in the rock section that overlies basement vary from about 3.5 km/sec at the base to 1.9 km/sec in the upper part.

LARSE line 2 crosses the extrapolated offshore location of the Palos Verdes Fault just northeast of Santa Monica

Canyon, and this seismic section does show a fault that cuts rocks close to shore. This fault might correlate with the Palos Verdes Fault, as proposed by ten Brink *et al.* (2000), but the fault revealed by the seismic section lies within the zone of west-striking faults that are related to the development of the Transverse Ranges. This fault might instead be the Santa Monica or a related fault (Fig. 1).

Two small-air-gun sections (numbered 39B and 41 in Fig. 7) intersect in northeastern Santa Monica Bay and show geology that is similar to that evident on LARSE line 2. In both sections, the location of Santa Monica Canyon coincides with the seafloor outcrop of apparently north-dipping rocks that return strong, continuous reflections. These rocks could be Miocene volcanic rocks or metamorphic basement. Where rock-velocity data are absent, the north-dipping reflection might cap strongly folded sedimentary rocks.

A structure that may play an important role in the offshore geology lies just northwest of Santa Monica Canyon,

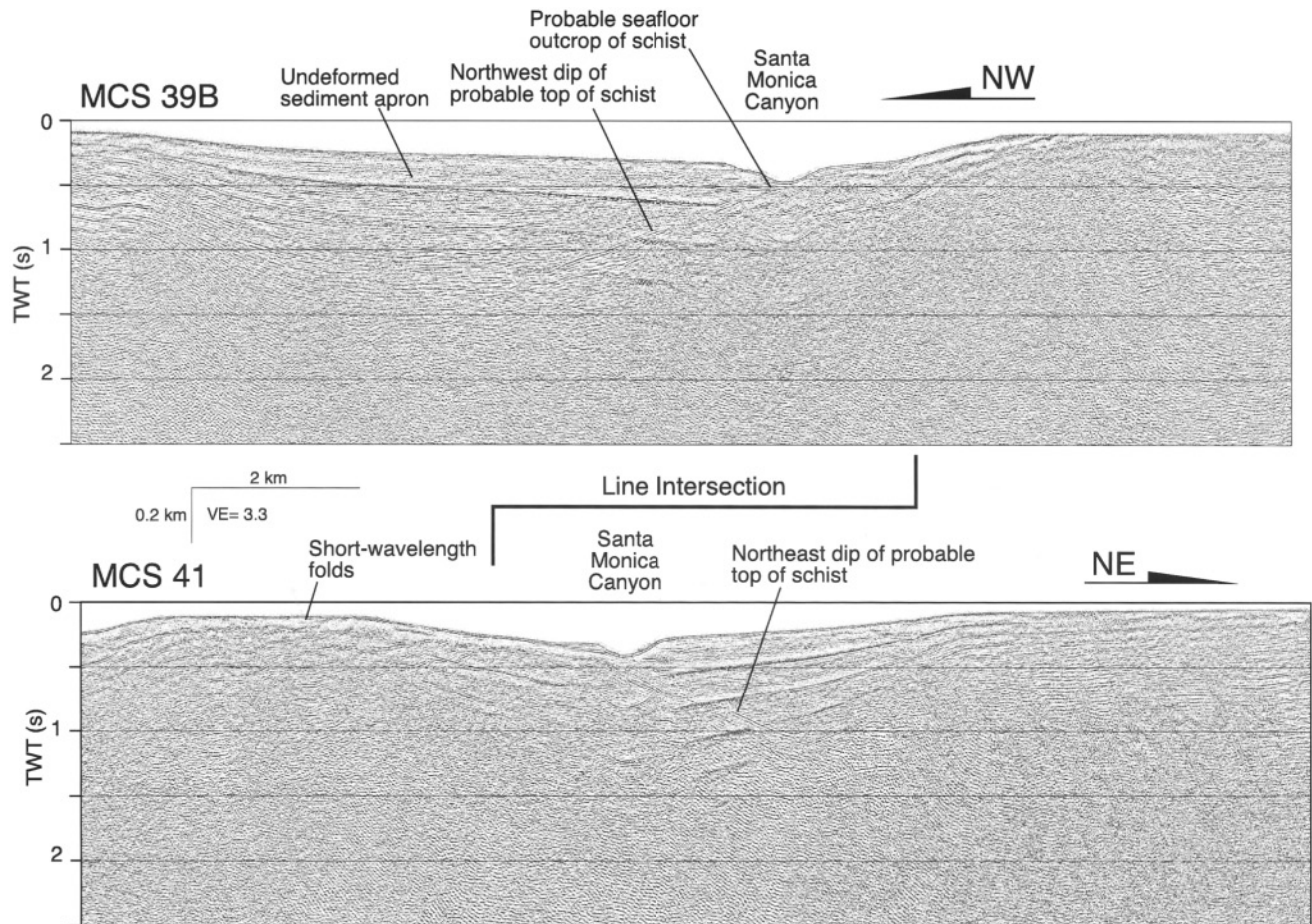


Figure 7. Poststack-migrated MCS sections collected in the northeast part of Santa Monica Bay. Section locations shown in Figure 4. Northwest and northeast-dipping reflections indicate the top of acoustic basement. Rocks that cause these reflections appear to crop out along the wall of Santa Monica Canyon. No obvious reflections or disrupted reflections indicate the location of the Palos Verdes Fault.

where an anticline (Figs. 3 and 8) has the west strike of faults that make up the Santa Monica Mountains instead of the predominant northwest strike of structures to the south. (We note that seismic-reflection line 10 [Fig. 8] is among a group of lines plagued by a high noise level that originated in the recording system. The northern gray area in Fig. 3 shows the part of the margin where the geology is difficult to discern through such noise.) This anticline folds complicated stratigraphic units associated with Santa Monica Canyon (Fig. 8), so the fold's history of development is difficult to decipher, but this fold's strike is well established, on the basis of the number and location of seismic-reflection lines available to us (Fig. 2).

The west-striking anticline (Fig. 8) underlies a sector of the continental margin where an embayment of the continental slope extends eastward and is bounded on the south-southeast by Santa Monica Canyon (see bathymetry in Fig. 1). Seismic-reflection data show that at least the upper part of the sediment apron underlying this slope has undergone little recent deformation (Fig. 8).

This low degree of deformation contrasts greatly with the tight folding of rocks under the shelf south of Santa Monica Canyon. This folding affects rocks within the shelf projection anticlinorium (Nardin and Henyey, 1978), and the folding extends eastward nearly to the location of the Palos Verdes Fault. Typically within the area outlined in Figure 3, rocks are deformed into numerous short-wavelength (>500 m) folds that are truncated at the seafloor. Individual folds cannot be correlated between seismic-reflection sections to obtain axial trends, but this folding style underlies most of the continental shelf between the Santa Monica and Redondo Canyons.

Another contrast in the geology on opposite sides of the Santa Monica Canyon involves the depth to the metamorphic basement. In general, north of this canyon, basement is below the reach of our small-air-gun system, except in the northeast corner of Santa Monica Bay, where dipping basement reflections were recorded (Fig. 7). In contrast, south of this canyon, basement is at shallow depth, less than 1 km (see also ten Brink *et al.*, 2000). Large-air-gun MCS data

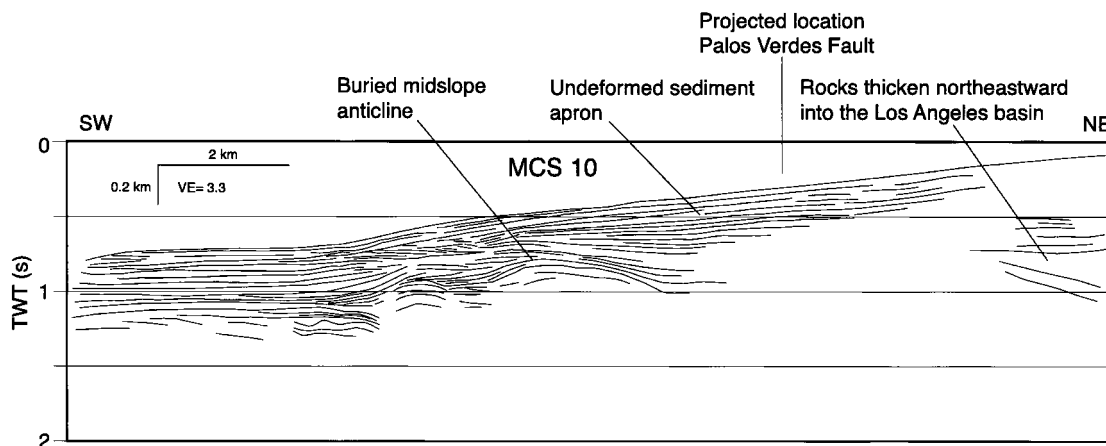


Figure 8. Line drawing interpreted from poststack-migrated MCS section 10. The location is shown in Figure 4, showing the undeformed sediment apron that extends across the projected location of the Palos Verdes fault. The indicated midslope anticline strikes nearly west and is located about 10 km northeast of the northwest-striking anticlines under the lower slope (Fig. 3).

collected for LARSE (line 2, Fig. 6a) do not show reflections from below the basement reflection that is also evident in small-air-gun data.

An important point is that none of our seismic-reflection sections, like those in Figures 6, 7, and 8, reveal features that point unequivocally to the location of the Palos Verdes Fault. Seismic-reflection section 39B (Fig. 7) reveals a shallow, undeformed sediment apron across the projected location of the Palos Verdes Fault, as does seismic line 10 (Fig. 8). This absence of near-surface fault expression in geophysical data contrasts with the situation southeast of the Palos Verdes Peninsula. Seismic and multibeam bathymetric data collected in the southeastern area have been interpreted to suggest that the Palos Verdes Fault can be followed across the shelf and slope (Fischer *et al.*, 1987; Greene and Kennedy, 1987; Marlow *et al.*, 2000).

Near the Palos Verdes Peninsula, none of the small-air-gun lines actually crosses the Palos Verdes Fault because the State of California effectively prohibits surveying with an air gun any closer than 3 miles from shore. However small-air-gun seismic lines that cross the continental shelf show that the wavelength of shallow folds increases irregularly eastward across the shelf toward the projected location of the Palos Verdes Fault. Short-wavelength folding ends in the northeast about 2 km from the fault's proposed location. Seismic-reflection section 45 (Fig. 9) reveals that within 2 km of the fault's projected location, strata are deformed into a broad, open fold. Similarly, MCS line 102 (Fig. 9) shows that the short-wavelength folding underlies but does not disturb a thick section of channel fill. Dating the oldest units of this fill would put an upper limit on the age of folding that affected an extensive area of the continental shelf. In any case, this folding ends south of the projected location of the Palos Verdes.

We collected Geopulse seismic-reflection across the

projected location of the Palos Verdes Fault (Fig. 10). The Geopulse system uses high-frequency sound, so it reveals only features within the upper few meters of sediment. With these limitations, we would only be able to identify very recent fault movement. The Geopulse section located in the southeastern corner of the study area, adjacent to the Palos Verdes Peninsula (line 602, Figs. 10, 11), shows the flank of Redondo Canyon and the flat continental shelf. The high topography near this canyon head impedes the analysis of offshore structural features; even so, the seafloor is not offset near the projected location of the Palos Verdes Fault. The next Geopulse line to the northwest (line 101, Fig. 11) reveals locally complicated stratigraphy (in the middle of the section, just below 0.1 sec) that might be related to fault movement. However an unconformity overlying the complicated stratigraphy is not offset or deformed, neither is the seafloor. This unconformity is undated, but we speculate that it was cut during the last glacial maximum, and so it dates from about 12 ka ago. If the underlying, complicated stratigraphy results from movement along the Palos Verdes Fault, then an important goal of future studies will be to date the unconformity to constrain the time of youngest fault movement.

Neither Geopulse section 43 nor 45 (Fig. 11) shows any offset of the seafloor along the projected strike of the Palos Verdes Fault. Both sections include poor data and reveal only discontinuous reflections from south-dipping strata, but these data are good enough to rule out the presence of measurable, vertical separation along a fault. Geopulse section 41 (Fig. 11) reveals mainly little-disturbed strata at the projected location of the Palos Verdes Fault, which would be located under the slope that leads downward into Santa Monica Canyon.

The Redondo Canyon Fault has been proposed (e.g., Nardin and Henyey, 1978; Wright, 1991) to follow Redondo

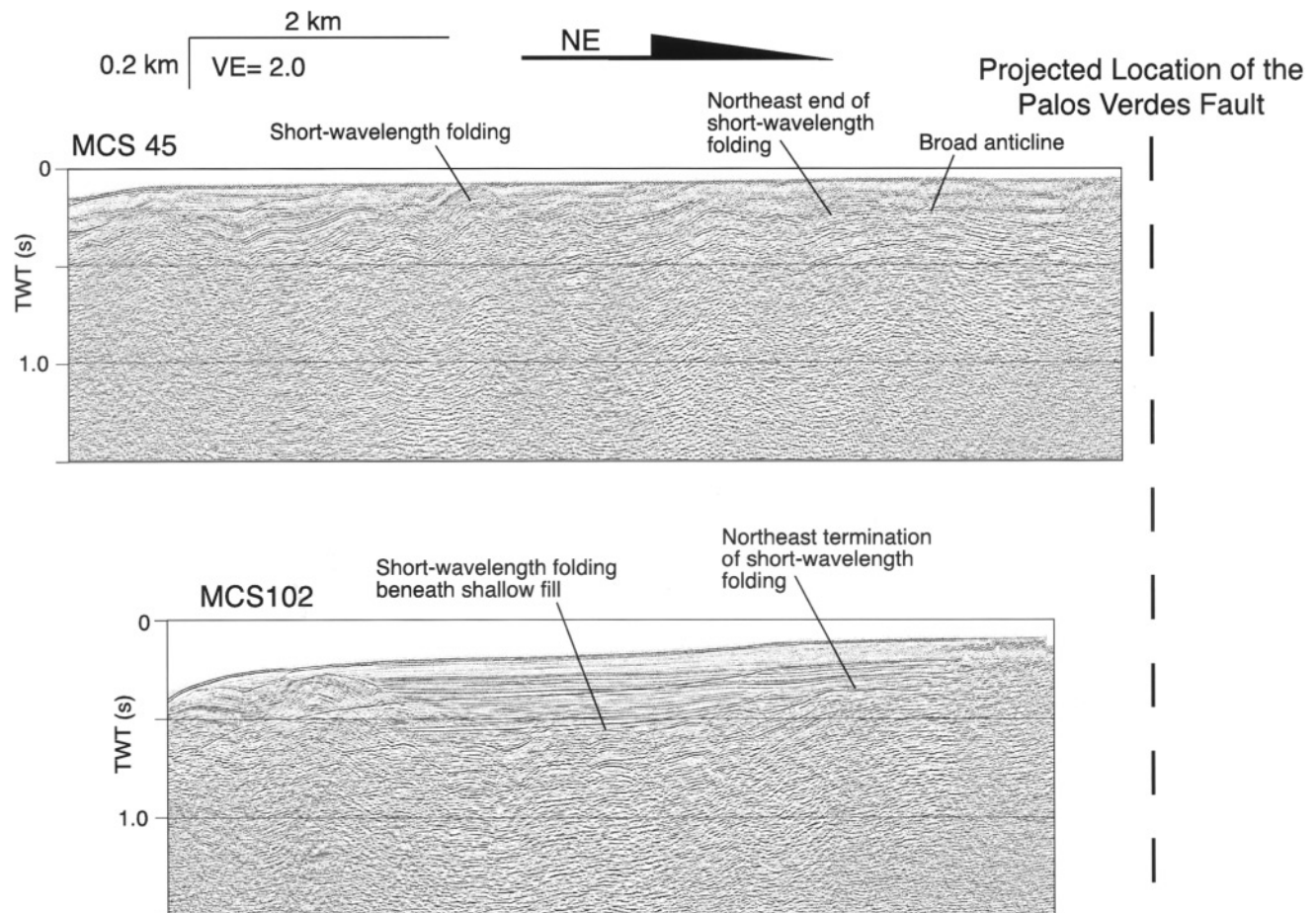


Figure 9. Poststack-migrated MCS sections collected in southeastern Santa Monica Basin. Section locations are shown in Figure 4. These two seismic sections nearly cross the Palos Verdes Fault near shore. They show the geologic structure near this fault, in particular the short-wavelength folding that affects shelf rocks over a broad area south of Santa Monica Canyon. Geopulse data collected across the projected fault location, from previous studies, are shown in Figure 11.

Canyon southwestward across the continental shelf (Fig. 3). Seismic-reflection sections across this proposed fault (Fig. 12) do not show clear reflections from a low-angle fault plane, and the short streamer used to record seismic-reflection data used here would not detect reflections from a steeply dipping fault.

Strata in what would be this fault's upper plate, along the south side of Redondo Canyon, are deformed by faults and short-wavelength folds that are similar in appearance to the folds under the shelf to the north. This complicated deformation probably masks the presence of a fault.

Structure Related to the San Pedro Escarpment

The San Pedro Escarpment marks an important geologic boundary between the basement ridge under Santa Monica Bay and the deep-water (500 m) Santa Monica and San Pedro Basins (Figs. 1 and 10). As we use the term here, the "San Pedro Escarpment" refers to the seafloor declivity that extends southeastward from Santa Monica Canyon to the

area southeast of the Palos Verdes Peninsula. Thus the escarpment extends for nearly 60 km along the southern California margin and attains its sharpest expression, nearly 700 m of relief with a 10° seafloor slope, adjacent to the Palos Verdes Peninsula. Beneath the escarpment, sedimentary rocks of probable Quaternary age (Greene and Kennedy, 1987; Vedder, 1990) dip and thicken to the southwest, into the deep-water basins. Along much of the escarpment's length in the study area, active folds and faults cut the seafloor and mark the escarpment's foot (Fig. 3).

At Santa Monica Canyon, the San Pedro Escarpment hooks to the north and east and merges with the steep southeast canyon wall (Fig. 1). This abrupt turn forms a prominent bathymetric nose that marks the northwest termination of the shelf projection anticlinorium. Two lower-slope anticlines having seafloor expression continue along the escarpment's general northwest strike toward Point Dume (Fig. 3). A shaded-relief image of the seafloor derived from multibeam bathymetric data (Fig. 10) (Gardner and Dartnell, 2002)

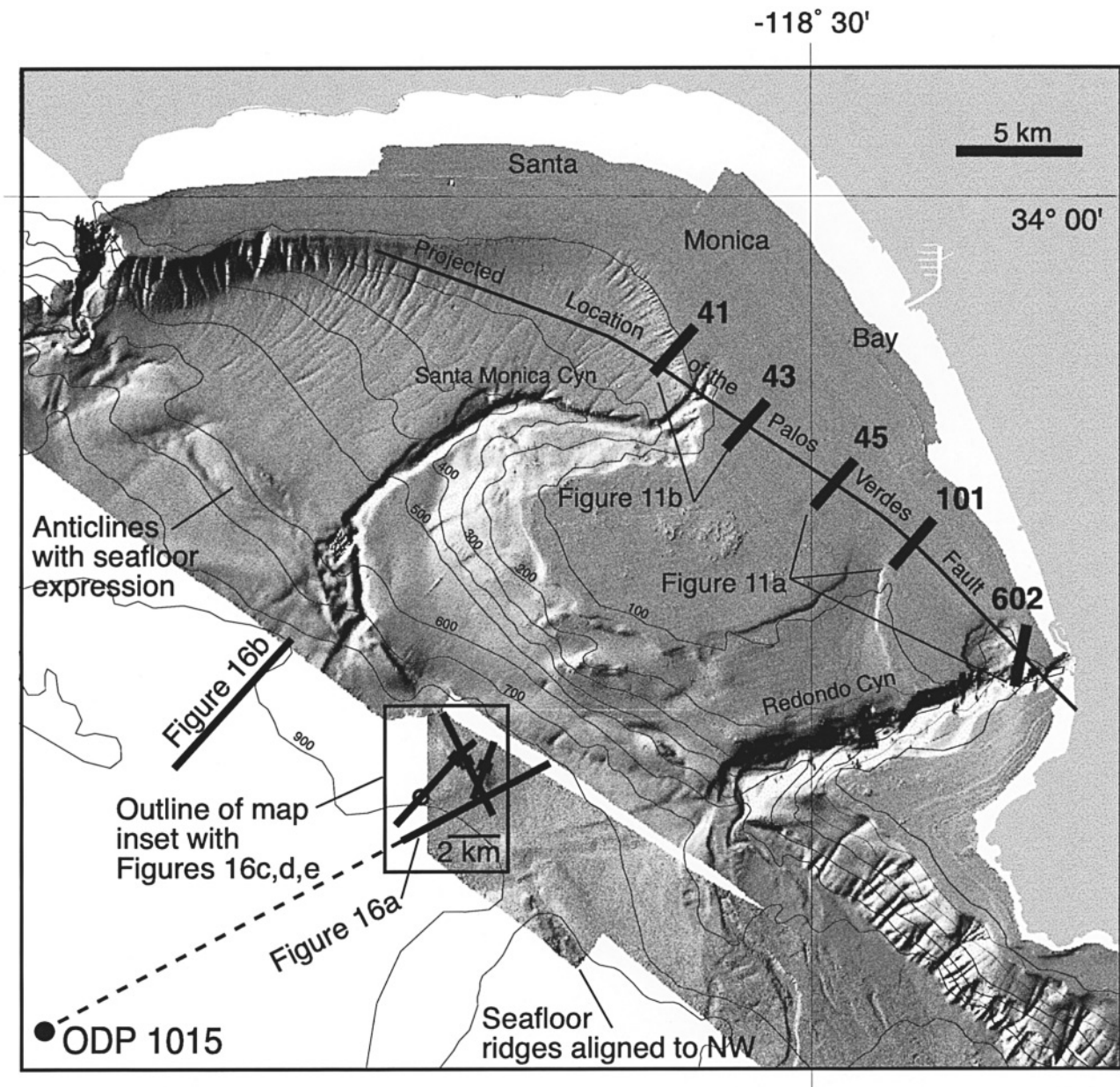


Figure 10. Location map for Geopulse and Huntec deep-tow boomer sections shown in Figures 11, 15, and 16. The dashed line shows the southwest extension of the profile segment of Figure 16a to indicate the direct tie to ODP site 1015. Shaded relief map of offshore area is made from multibeam bathymetric data that are viewed from directly overhead and illuminated from the northwest (Gardner and Dartnell, 2002). Anticlines evident in seafloor relief in the northwest part of the area are shown in cross section in seismic sections 51 and 52 (Fig. 13). Seafloor ridges cross the basin plain in the southeast part of the study area and are shown in cross section in Figure 16.

shows these anticlines and a southeastward jog in the Santa Monica Canyon that is probably structurally controlled.

Structures marking the base of the continental slope and the San Pedro Escarpment change markedly in style where Santa Monica Canyon crosses the escarpment. For this reason we divide the lower slope into two sectors: one extends southeastward from Point Dume to the canyon, and the second spans from this canyon to the Palos Verdes Peninsula.

In the first sector, seismic-reflection section 52 (Fig. 13) reveals two lower-slope anticlines that have clear seafloor expression. The northeast flank of the upslope anticline is cut by a fault showing reverse separation. These subparallel anticlines are continuous along the lower slope from near Point Dume to Santa Monica Canyon (Fig. 3).

The downslope anticline (Fig. 13, line 52) begins in the northwest as two or more thrust faults that deform shallow

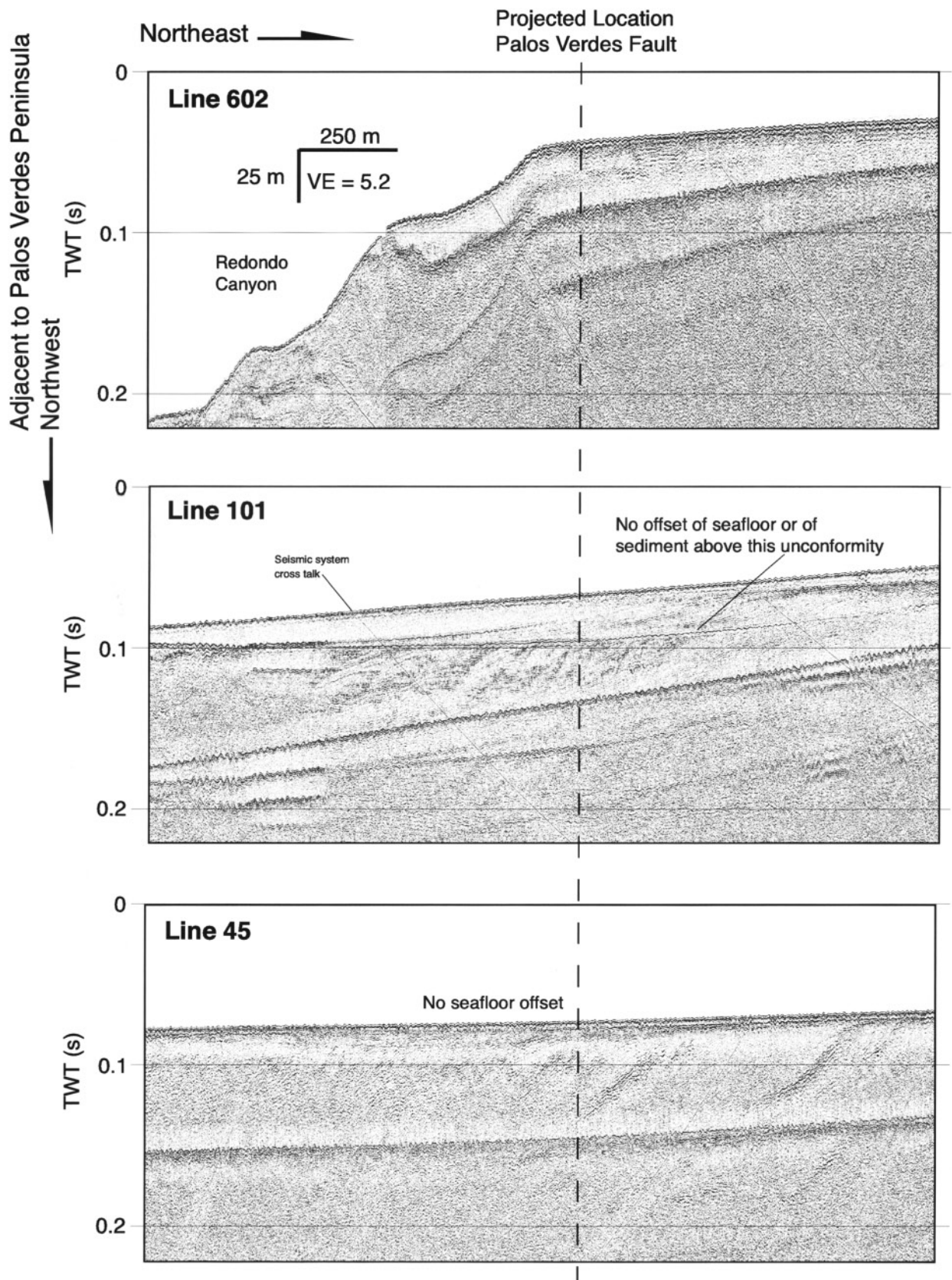


Figure 11. Caption on facing page.

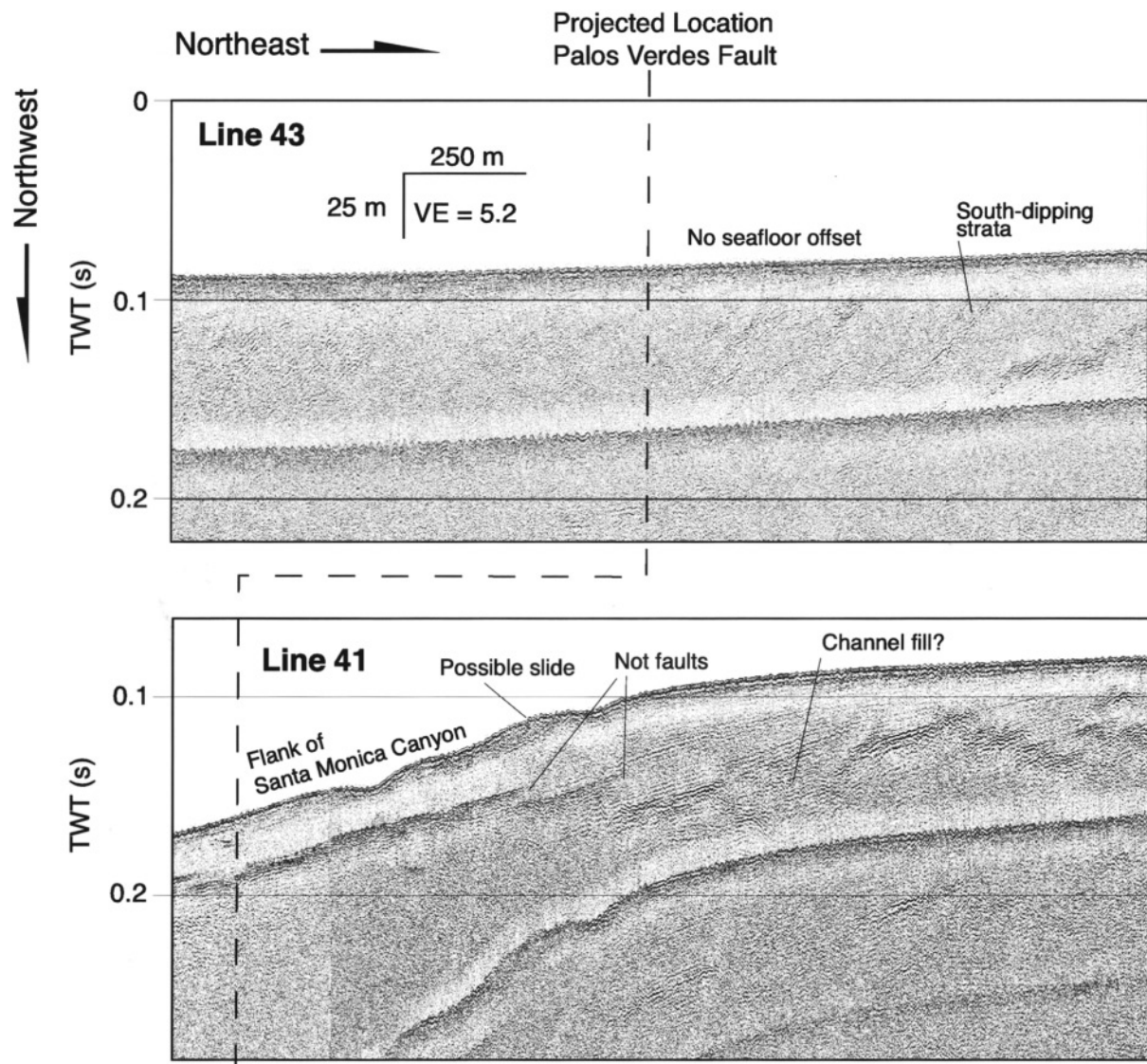


Figure 11. Geopulse seismic data collected over the projected location of the Palos Verdes Fault. Features on section 41 labeled “Not faults” instead show the effects of gain changes during seismic acquisition. Section locations are shown in Figure 10.

rocks in the Santa Monica Basin (Fig. 3). Southeastward along strike, these faults coalesce and the downslope anticline gains structural relief over a short distance. The two lower-slope anticlines are then coextensive for more than 20 km along the foot of the continental slope. The anticlines attain their greatest structural relief, about 200 m, below seismic lines 51 and 52 (Fig. 13).

The two lower-slope anticlines were active recently, as shown by their seafloor expression along almost the entire length of both folds, by the shallow basin fill that thins into the fold limbs, and by the concordant folding of all but the shallowest fill. The structural asymmetry, particularly of the northeastern fold evident in MCS line 52 (Fig. 13), reveals a northeastward structural vergence.

Rapid growth of these anticlines is suggested by the

truncated reflections, near the anticlinal crest (Fig. 13, inset detail 1 of line 51), that underlie continuous reflections from arched strata. Both truncated and arched reflections are folded to nearly equal degrees. We interpret this reflection sequence to mean that during early fold growth, sediment near the fold crest became unstable and was shed into the basin, leaving the truncated reflectors, but overlying strata was deposited over the truncated reflectors and then arched without failure. Seismic-reflection section 52 (Fig. 13) shows that recent structural growth has been vigorous enough that some of the sediment has been shed from near the fold’s crest.

Toward Santa Monica Canyon, the two lower-slope anticlines converge and diminish in structural relief (Figs. 3 and 13). Near the mouth of this canyon the anticlines are

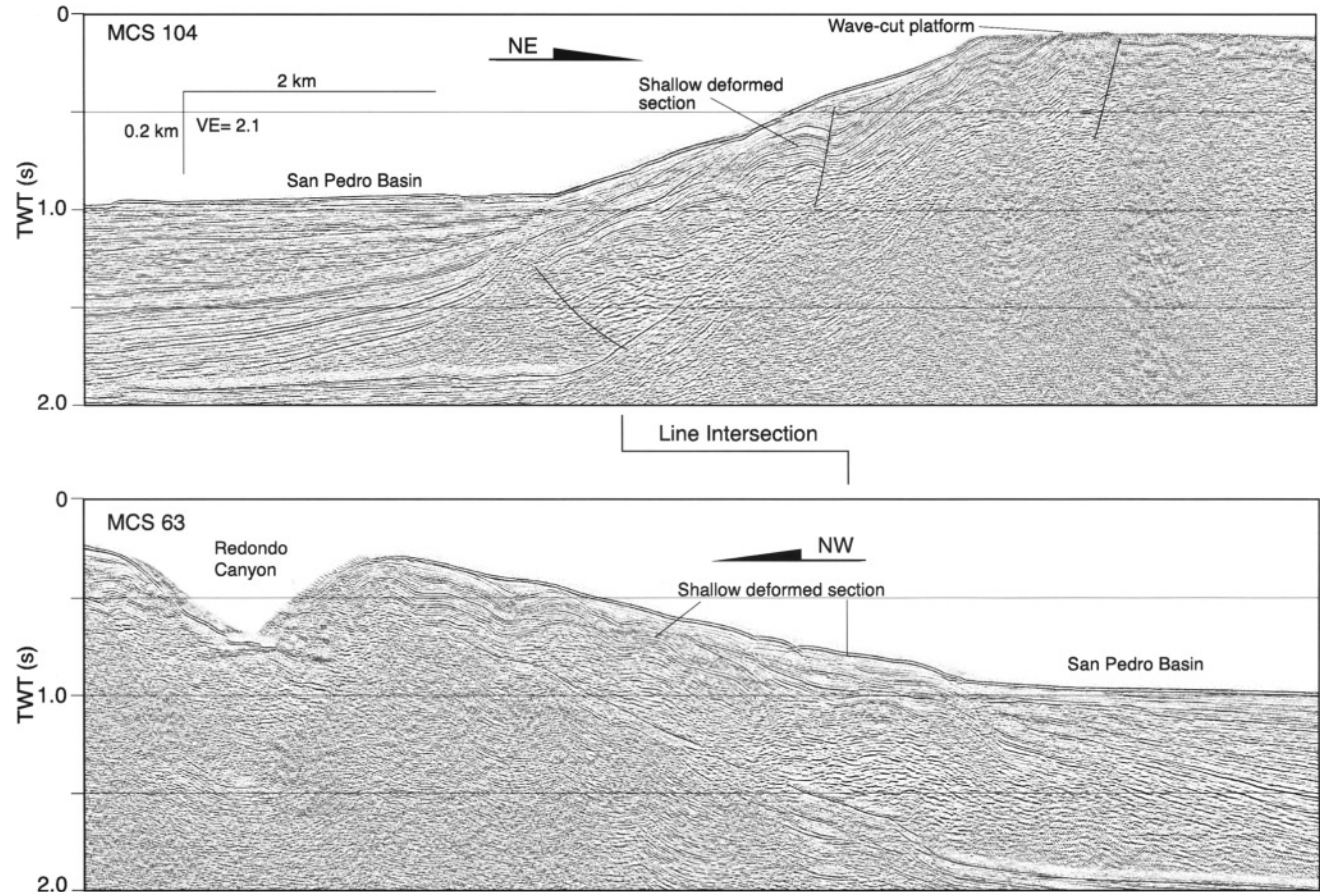


Figure 12. Poststack-migrated MCS sections, which cross the upper plate of the proposed Redondo Canyon Fault. Section locations are shown in Figure 4.

replaced to the southeast by the steep San Pedro Escarpment and its underpinning structures.

The second sector of the escarpment stretches southeastward from Santa Monica Canyon to near the Palos Verdes Peninsula. Faults and folds deform rocks under the escarpment, and some faults extend upward nearly to the seafloor, indicating recent deformation (Fig. 14). The lower-slope anticlines deform Pleistocene sediment that makes up much of the Santa Monica fan. A fault offsets the strong reflector (labeled "AB" [acoustic basement] in Fig. 14) at the base of the sedimentary section near the northeast ends of seismic-reflection sections 48 and 41. The strong reflector dips southwest under the escarpment, and because of the high refraction velocities measured along the LARSE MCS streamer, this reflector is probably the top of metamorphic basement or of Miocene volcanic rocks.

Faulting intensifies southeastward for about 10 km along the San Pedro Escarpment, as illustrated by the group of reflections labeled "a" in seismic-reflection sections on Figure 14. In section 49 (Fig. 14, top), the "a" reflections are broadly folded above a fault showing reverse separation. These reflections dip progressively steeper to the southeast (compare sections 49 and 48 in Fig. 14). In section 41, the

main fault has accrued marked (about 30-m) seafloor expression (section 41; Fig. 14).

This structural relief decreases sharply southeastward. In section 42 (Fig. 14, bottom) faulting has reduced intensity, the main faults are nearly vertical and form a simple flower structure, and the seafloor expression of the fault zone has dwindled to a small high. The shaded-relief image of the seafloor derived from multibeam bathymetric data (Fig. 10) shows that small seafloor highs, like the one just described, fall along a northwest-trending lineament that marks the location of the San Pedro Basin fault zone (Fig. 3). The lineament extends northwest nearly to intersect with the Santa Monica Canyon.

The nearly vertical fault on section 42 (Fig. 14) is the San Pedro Basin fault zone, which is thought to be an oblique slip fault. We discuss this fault in more detail later, in the section concerning the Santa Monica and San Pedro Basins. We also note that the intensity of folding under the San Pedro Escarpment decreases southeastward to where seismic lines 43 and 44 (Fig. 15) cross the escarpment. In general, structures deforming lower-slope and basin rocks spread out and lose relief or were more rapidly buried to the southeast.

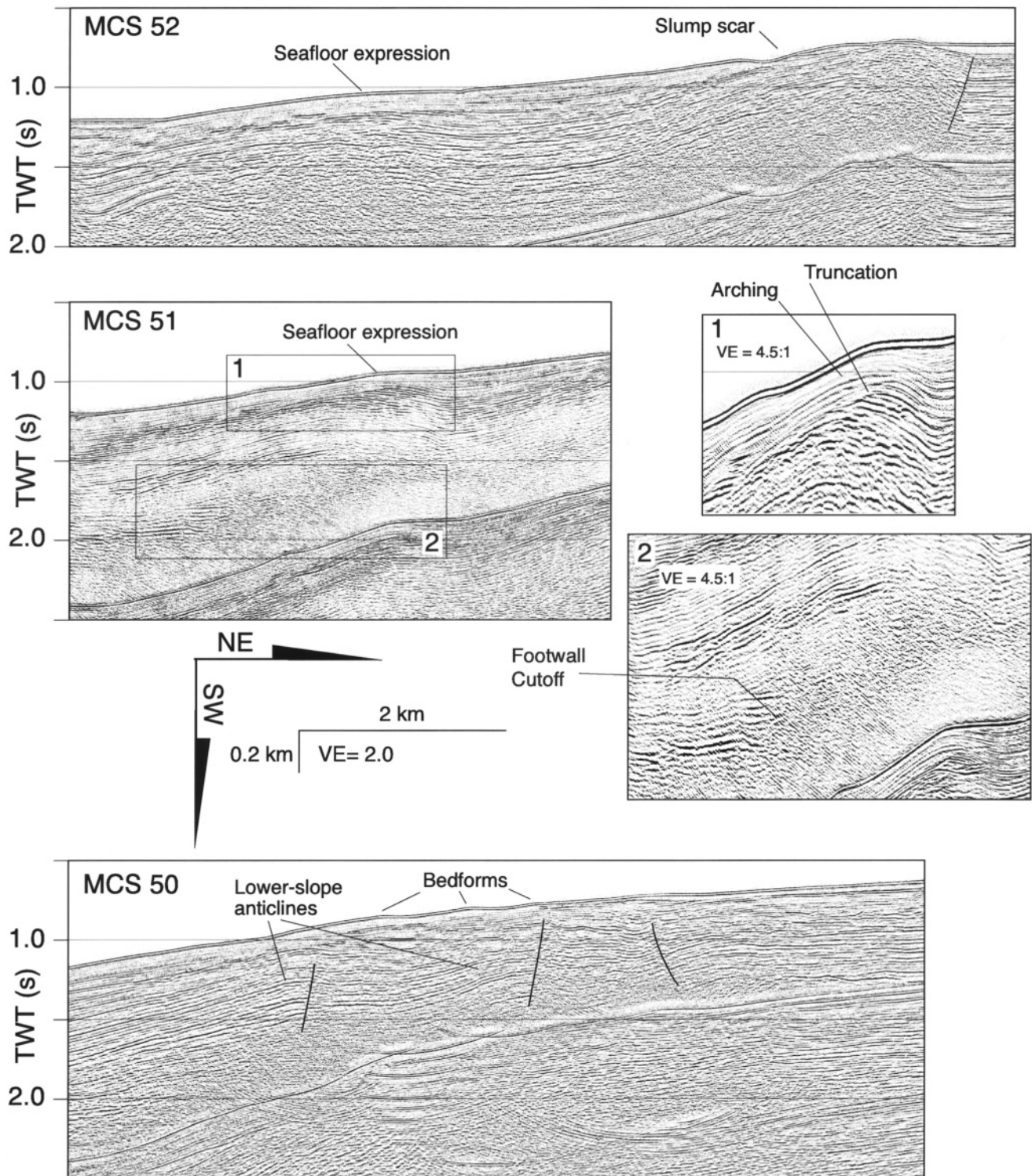


Figure 13. Poststack-migrated MCS sections over the lower-slope anticlines that extend southwest from near Point Dume to near the northwest end of the San Pedro Escarpment. Section locations are shown in Figure 4. Detailed section 1 shows strata over the crest of the northeastern anticline that were truncated, possibly by slumping or erosive turbidity currents, during early folding. Detail section 2 shows the geometry of beds in one anticline, which appear to have been deformed by a thrust fault. Section 50 shows the anticlines near Santa Monica Canyon, where they die out.

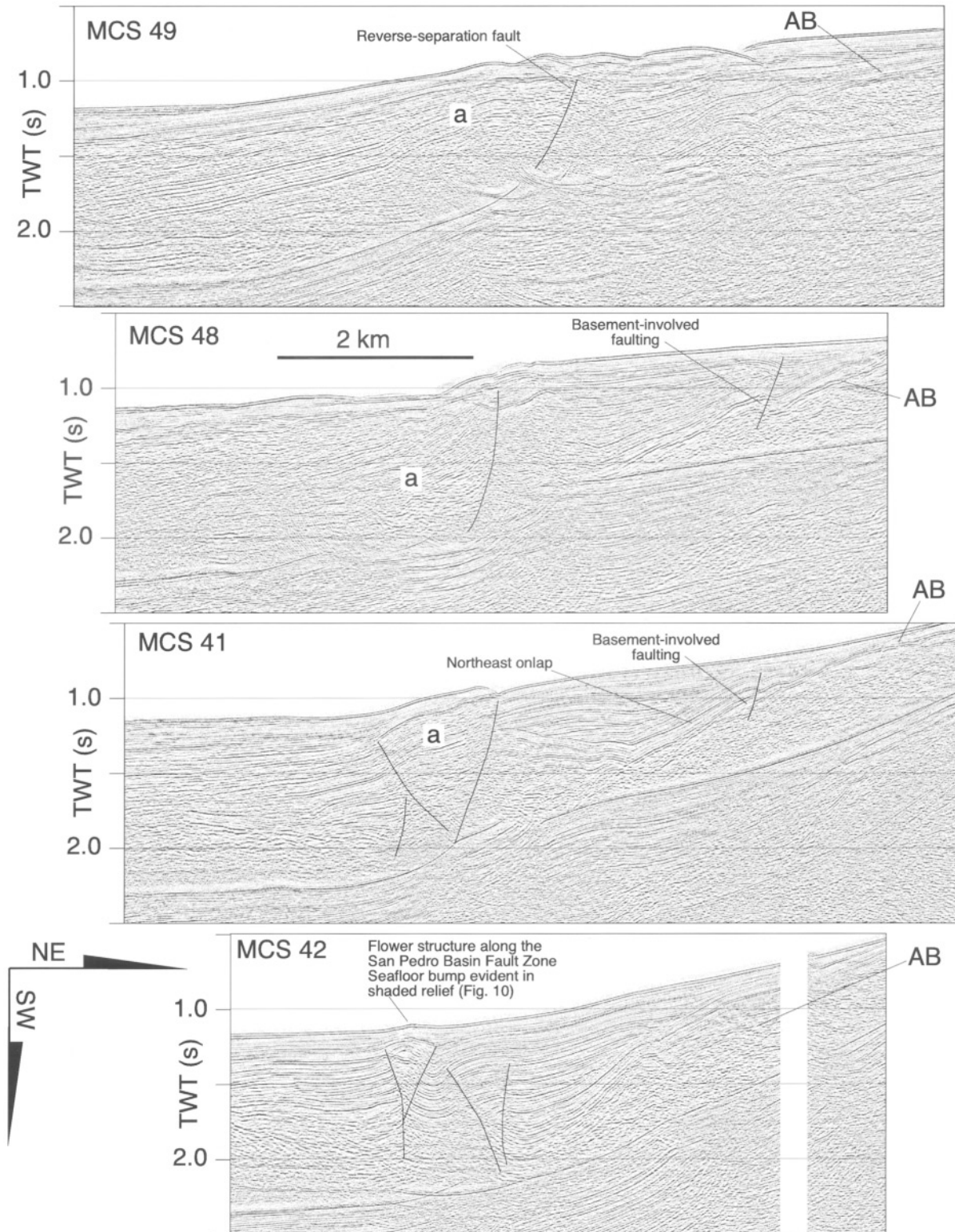


Figure 14. Poststack-migrated MCS sections, location shown in Figure 4, illustrating the geologic structure of the San Pedro Escarpment southwest of Santa Monica Canyon. Strata indicated by the "a" dip more steeply to the southwest on section 48 than elsewhere. Faults offset what is believed to be the reflection from acoustic basement (AB), which is probably made up of metamorphic rocks. The flower structure along the San Pedro Basin fault zone is distorted in part by migration noise.

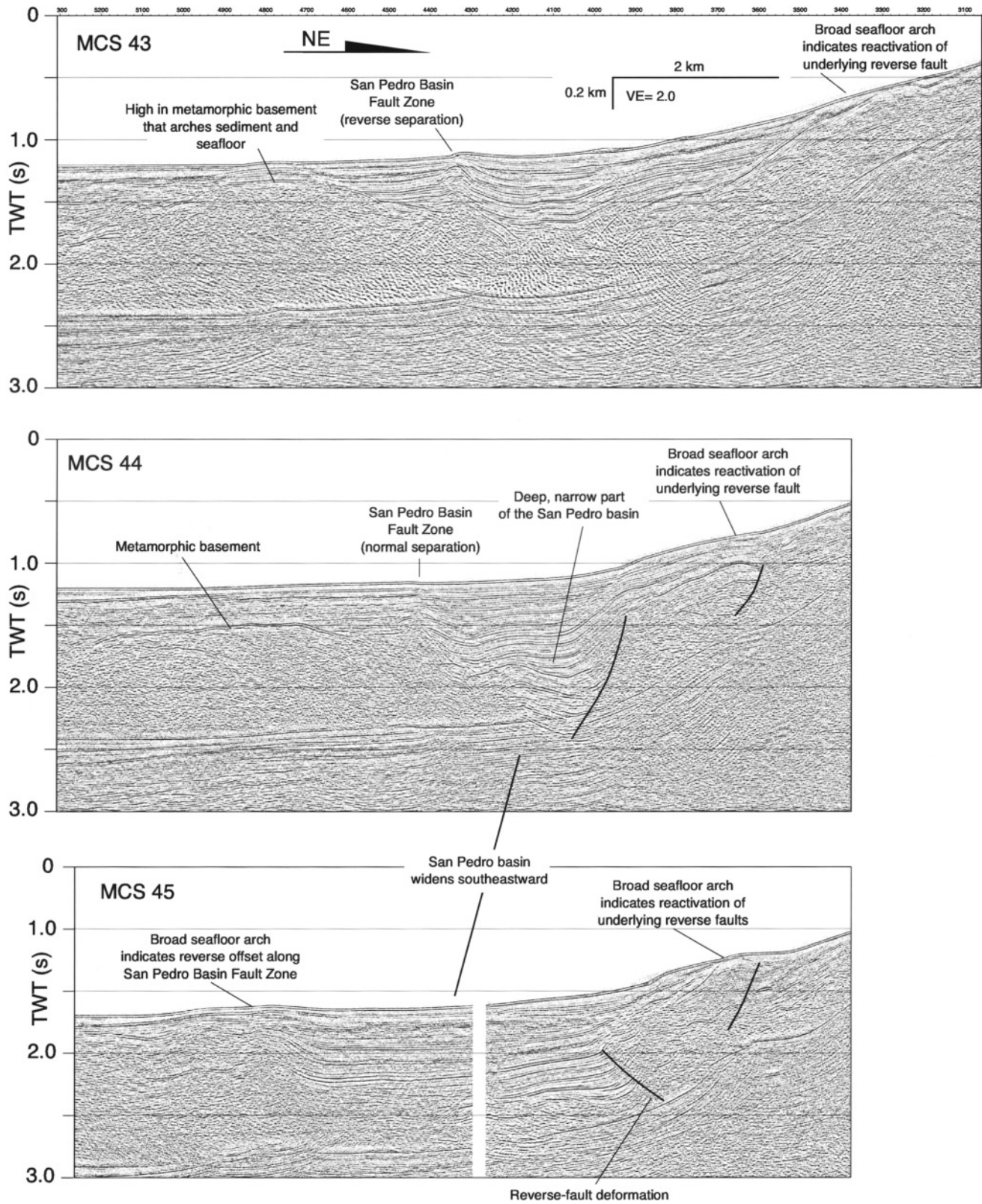


Figure 15. Three poststack-migrated MCS sections, showing the structure of the Santa Monica Basin between the San Pedro Escarpment, on the east, and acoustic-basement features that recently arched the seafloor, on the west. Locations of sections shown in Figure 4.

This evolution in structural style along the San Pedro Escarpment mirrors changes in the width and depth of the San Pedro and Santa Monica Basins. Convergent or transpressive structures evident in the northwest, on section 48 (Fig. 14), are located where the Santa Monica Basin is wide and deep (Fig. 1). These structures evolve southeastward into a flower structure, as on section 42 (Fig. 14). Farther southeastward, as shown by seismic section 44 (Fig. 15), the San Pedro Basin is narrow and deep, and nearby convergent structures have low relief. LARSE seismic sections 2 and 3 (Fig. 6) cross over the San Pedro Basin (Fig. 2) and show that this narrow basin lies between shallow basement rocks on the south and the escarpment on the north. Section 45 (Fig. 15) reveals that the San Pedro Basin is wider and deeper than it is to the northwest, and most nearby structures have low relief. Section 45 also shows that the northeast side of the San Pedro Basin is deformed by faults showing reverse separation.

Along the San Pedro Escarpment, then, compressive and extensional structures are commingled and have a complex distribution that, in some aspects, is difficult to envision even from the relatively close-spaced seismic sections we used. This commingling and the flower structure on seismic section 42 (Fig. 14) underscore the importance of strike-slip faulting on the development of structures along the escarpment and within the San Pedro Basin.

Age of Structural Development

Dating the development of the complex structures along the San Pedro Escarpment is important for the evaluation of the regional earthquake hazard. Constraints on timing come from correlating seismic-reflection data, collected with a high-resolution deep-towed boomer system, with the stratigraphic record obtained from ODP site 1015 (Shipboard Scientific Party, 1997; Normark *et al.*, 1998). The seismic section shown in Figure 16a is part of a larger section that extends southwest from the San Pedro Escarpment, across the Santa Monica Basin, and through the ODP drill site (dashed line in the lower-left corner of Fig. 10). Coring at this site recovered 150 m of dominantly turbidite sediment fill; the rate of deposition during the Holocene averaged about $2.5 \text{ m}/10^3 \text{ yr}$ (Piper and Normark, 2001). Much of the sediment section cored at site 1015 is part of the Hueneme Fan, which is fed from the Santa Clara River at the western end of Santa Monica Basin (Normark *et al.*, 1998; Piper *et al.*, 1999). The dated reflectors J to O shown on Figure 16 are from the latest Pleistocene and Holocene; reflector J, for example, marks the last glacial low stand of sea level at the close of the Pleistocene (Piper and Normark, 2001). Dated horizons can be mapped across the entire eastern half of Santa Monica Basin.

Along the base of the continental slope, the flat-lying turbidites of the Hueneme Fan onlap and wedge against the lower slope (Fig. 16b). Sandy turbidite beds below reflector N wedge against the lower slope, and a condensed section

that blankets the slope itself represents the upper, muddy parts of these turbidite deposits. Above reflector N, the section is less muddy, and this latest Holocene section thins onto the lower slope without pronounced wedging. These dated reflectors have been correlated to folds that deform rocks at the base of the San Pedro Escarpment (Fig. 16a). Reflector J (13 ka old) (Fig. 16a) lies within the condensed section uplifted on the flank of the fold. Strata just a few meters below reflector J are deformed concordantly within the fold. Hence, the lower-slope folding began around the Pleistocene/Holocene boundary. Figure 16b shows that the sediment section between horizons L and J wedges against the lower slope. Reflector J (13.5 ka) onlaps a small, isolated, submarine-slide deposit that overlies a more extensive mass-wasting deposit with an irregular upper surface. The relief of this surface has been preserved by deposition of the latest Holocene sediment in hemipelagic drape (above horizon L). The date of these slides, just before 13 ka ago, is nearly the same as the age of the folding described earlier, suggesting that the two, outwardly independent processes of folding and sediment transport down a submarine canyon are linked and that with future work, they can be used to sharpen the timing of deformation.

Near the south limit of the shaded-relief map of the seafloor (Fig. 10), small ridges and knobs protrude above that seafloor and are aligned along a northwest trend. These seafloor features mark the location of the San Pedro Basin fault zone. They appear to be most evident west of the mouth of Redondo Canyon. Deep-tow boomer profiles that cross several of these features show when they formed. For example, the thickness of the turbidite section between J and M remains constant through the southwestern of the two folds (Fig. 16c; see also the detailed location and shaded relief map to the right of Fig. 16e). The section above reflector M thins northeastward, indicating that this fold began forming along the base of the slope more recently than 8 ka. Farther upslope, another fold appears to be faulted on its seaward flank. Our correlation of reflections through this fold suggests that folding began at about the time of reflector J (13 ka), about 5 ka earlier than the lower fold. The turbidite section between J and M wedges only slightly, suggesting that the early folding resulted in a low-amplitude structure. The seismic section profile in Figure 16b follows the crest of this northwest-trending fold; slight wedging of the section between reflectors J and L is observed along the margins of this feature.

A diapir punched upward through shallow basin fill (Fig. 16e), and the diapir is clearly evident as a bright, circular, seafloor projection in the shaded-relief map that is shown to the right of Figure 16e. The diapir is young, as indicated by the near absence of wedging in the sediment section above reflection J on the basinward flank of the diapir. Also the reflection character and spacing is similar on both sides of the diapir. The diapir indicates high-pressure fluids locally within the San Pedro Basin fault zone.

Structure of the Santa Monica and Northern San Pedro Basins

The deep-water Santa Monica Basin extends westward from the San Pedro Escarpment to the Santa Catalina Ridge, but small-air-gun seismic-reflection sections were collected only over the far eastern sector of this basin (Fig. 1). Small-air-gun MCS data do not show a reflection from basement because of masking by a strong, water bottom multiple. However large-air-gun MCS data from the U.S. Geological Survey 1990 and the LARSE 1994 surveys were obtained with sufficiently powerful acoustic sources to reveal the depth to basement. These data show that the Santa Monica Basin is extensive but shallow, being only about 1.5 km deep, and the basin overlies a strongly reflective, low-relief basement. This basement could include volcanic rocks but most likely comprises metamorphic rocks, the Catalina Schist, on the basis of wide-angle velocity data in ten Brink *et al.* (2000) and tomographic velocities in Figure 6b. Both velocity data sets reveal that beneath a sedimentary section about 1 km thick lie rocks having a seismic velocity of about 5 km/sec. The large-air-gun reflection data indicate that over wide areas southwestward from the Dume Fault, acoustic basement maintains a nearly constant depth below the seafloor. The basin pinches out to the southeast against the Redondo Knoll (Fig. 1), from which Miocene volcanic and volcanoclastic rocks have been dredged (Vedder, 1990).

Within the San Pedro Basin, the San Pedro Basin fault zone lies along or near the contact between basement rocks on the west and the basin's sedimentary fill to the east, and the separation across the fault varies considerably. For example, MCS section 46 (Fig. 17) shows reverse-fault separation, whereas the fault has normal separation in section 104. Folding along this fault is most pronounced deeper in the section; the horizon labeled "e" (section 104; Fig. 17) marks the top of the obviously folded basin fill. Folding above this horizon is subtle but affects rocks up to the seafloor, suggesting ongoing fault movement. The seafloor inflection indicated on section 46 is consistent with ongoing movement.

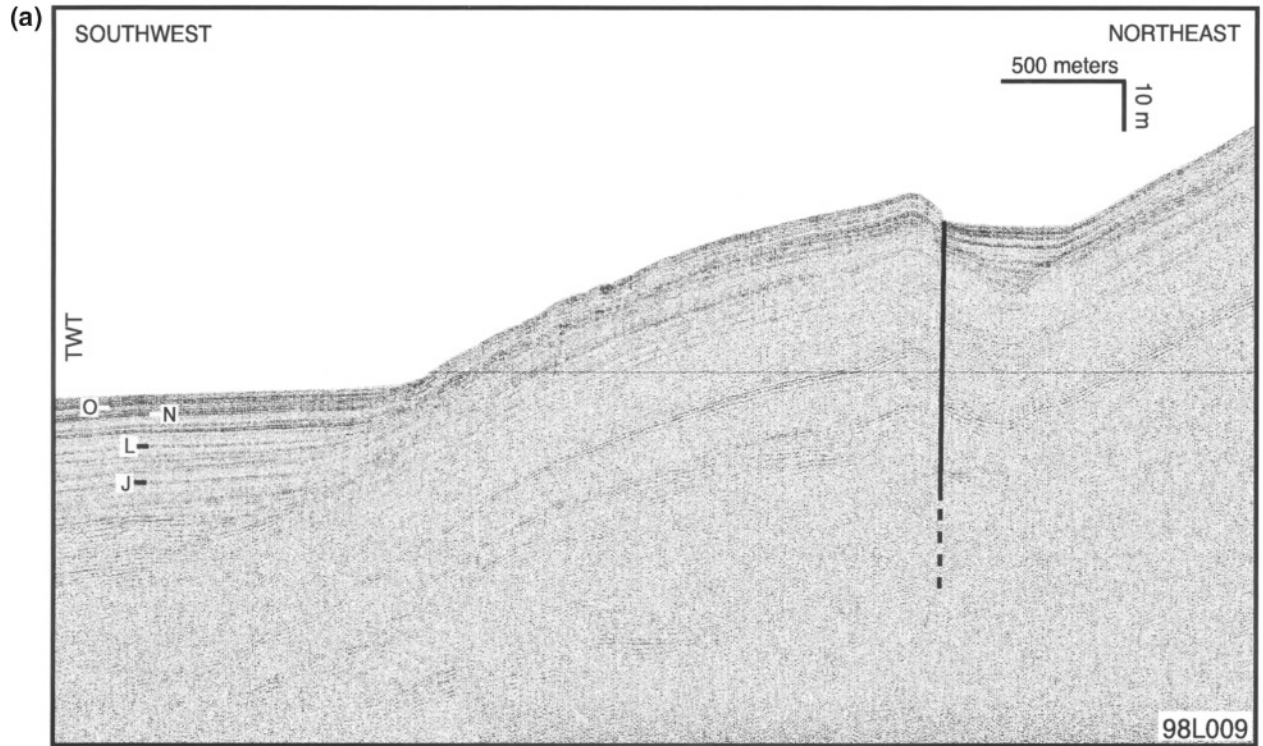
Discussion

The offshore geologic structure described falls within the tectonic crossroads below Santa Monica Bay, wherein northwest-trending faults, common southeast of this bay, somehow commingle with or are overprinted by west-striking faults associated with the western Transverse Ranges. In general, our seismic-reflection data reveal too little of the deep subsurface to delineate this structural convergence. Nonetheless, these data, together with regional geologic and seismological analyses presented elsewhere (e.g., Nardin and Henyey, 1978; Hauksson and Saldivar, 1986, 1989; Wright, 1991; McNeilan *et al.*, 1996; Dolan *et al.*, 2000), reveal that the Palos Verdes, Dume, and San Pedro Basin Faults should be included in analyses of regional earthquake

hazards, because within and near the study area, all of these faults show evidence for Quaternary movement.

Analyzing the earthquake hazard associated with the Palos Verdes Fault has been one of our primary research goals. An important question raised by this study is, What becomes of the Palos Verdes Fault northwest of the Palos Verdes Peninsula? Successive marine terraces show that near this peninsula, the fault has a high strain rate and is a likely source for earthquakes (Ward and Valensise, 1994). In addition, high-resolution seismic-reflection data collected onshore near this peninsula show what are interpreted to be strands of the Palos Verdes Fault at shallow depth (Stephenson *et al.*, 1995). However, marine Geopulse records obtained near Redondo Canyon (e.g., Fig. 11) reveal that this fault offsets neither the seafloor nor shallow sediment. This sediment probably was deposited since the last rise in sea level, beginning at about 12 ka. In part, the inability to chart the fault's location results from the repeated episodes of sub-aerial exposure and erosion of the shelf during the Pleistocene. One result of this erosion is that Quaternary sediment is not widely preserved on the shelf; thus the apparent absence of shallow faulted sediment may point to reduced Holocene faulting. Nardin and Henyey (1978) also mentioned that the offshore location of the Palos Verdes Fault is not evident in high-resolution seismic-reflection data they interpreted.

The Palos Verdes Fault may be associated with some structural and bathymetric features developed around the Santa Monica shelf, but with only limited success we tried to map the location and structure of the Palos Verdes Fault based on secondary features this fault may have caused. One possibility in this regard is that the Palos Verdes Fault forms the northeastern boundary of the shelf area that is underlain by rocks involved in the short-wavelength folding. As described earlier, these folds are part of the shelf projection anticlinorium (SPA in Fig. 1). They have wavelengths of about 500 m, they extend shoreward from the San Pedro Escarpment, and both the amplitude and wavelength of the folds tend to decrease northward and eastward away from the escarpment. Shelf rocks are folded primarily beneath the part of the shelf between the Santa Monica and Redondo Canyons (outlined in Fig. 3). The folding ends 5–10 km southwest of the offshore location of the Palos Verdes Fault that was proposed by other researchers (e.g., Yerkes *et al.*, 1965; Wright, 1992). The difference in position is most pronounced near Santa Monica Canyon, where the limit of folded rocks diverges from the fault's proposed location to follow approximately the canyon's south wall (Fig. 3). Seismic-reflection section 41 (Fig. 7), for example, shows that shelf rocks under the south canyon wall are folded, but under the opposite wall and northeastward away from the canyon, shelf rocks make up an undeformed sediment apron. Both seismic-reflection sections in Figure 7 show what are probably reflections from metamorphic basement. These basement rocks are not folded in the style evident across the canyon. Also basement rocks dip away from the canyon



Reflector ages from ODP Site 1015: O (1.5 ka), N (4.5 ka), L (9.5 ka), K (10.5 ka), J (13 ka)

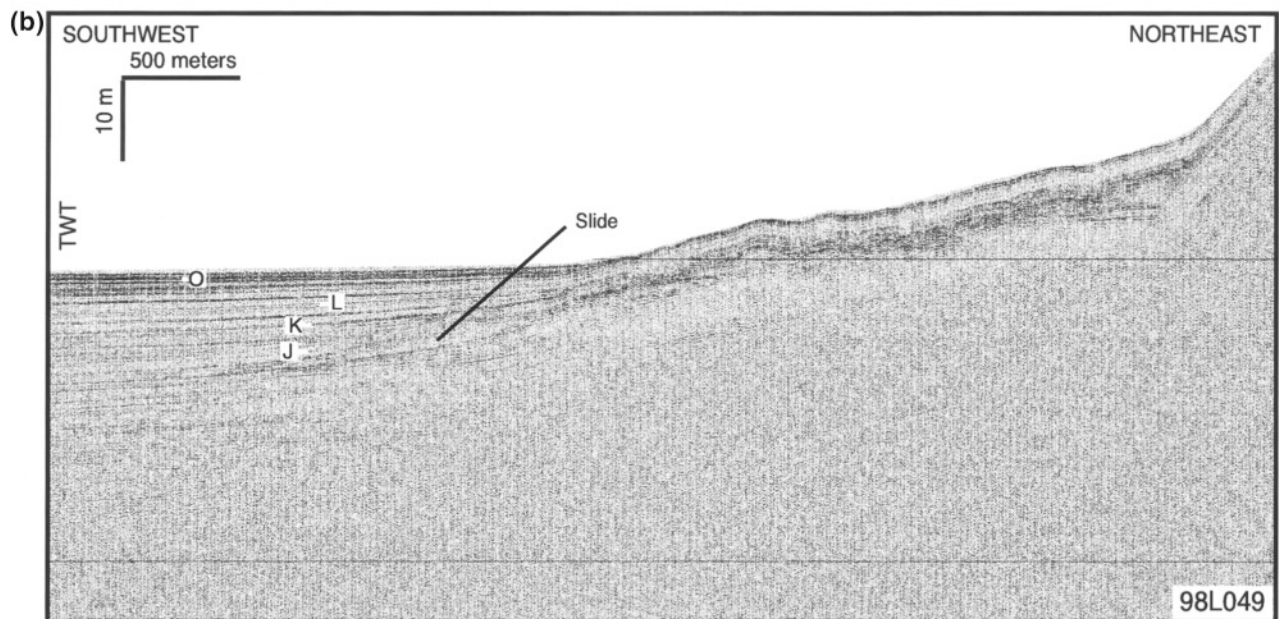


Figure 16. (a, b) Deep-tow boomer sections across the lower basin slope for which approximate ages can be derived from drilling results at ODP site 1015 (Normark *et al.*, 1998; Piper and Normark, 2001). Folding evident in Figure 15 (top) and sliding in Figure 15 (middle) seem to have begun before horizon J, which has been dated at 13 ka. Section locations are in Figure 10. (c–e) Deep-tow boomer sections across uplifted basin plain turbidites near the base of the Santa Monica slope. Key reflector stratigraphy from Piper and Normark (2001). Location of inset map shown in Figure 10. Diapir evident in the seismic section shown in Figure 16e is also evident as a narrow peak in shaded relief.

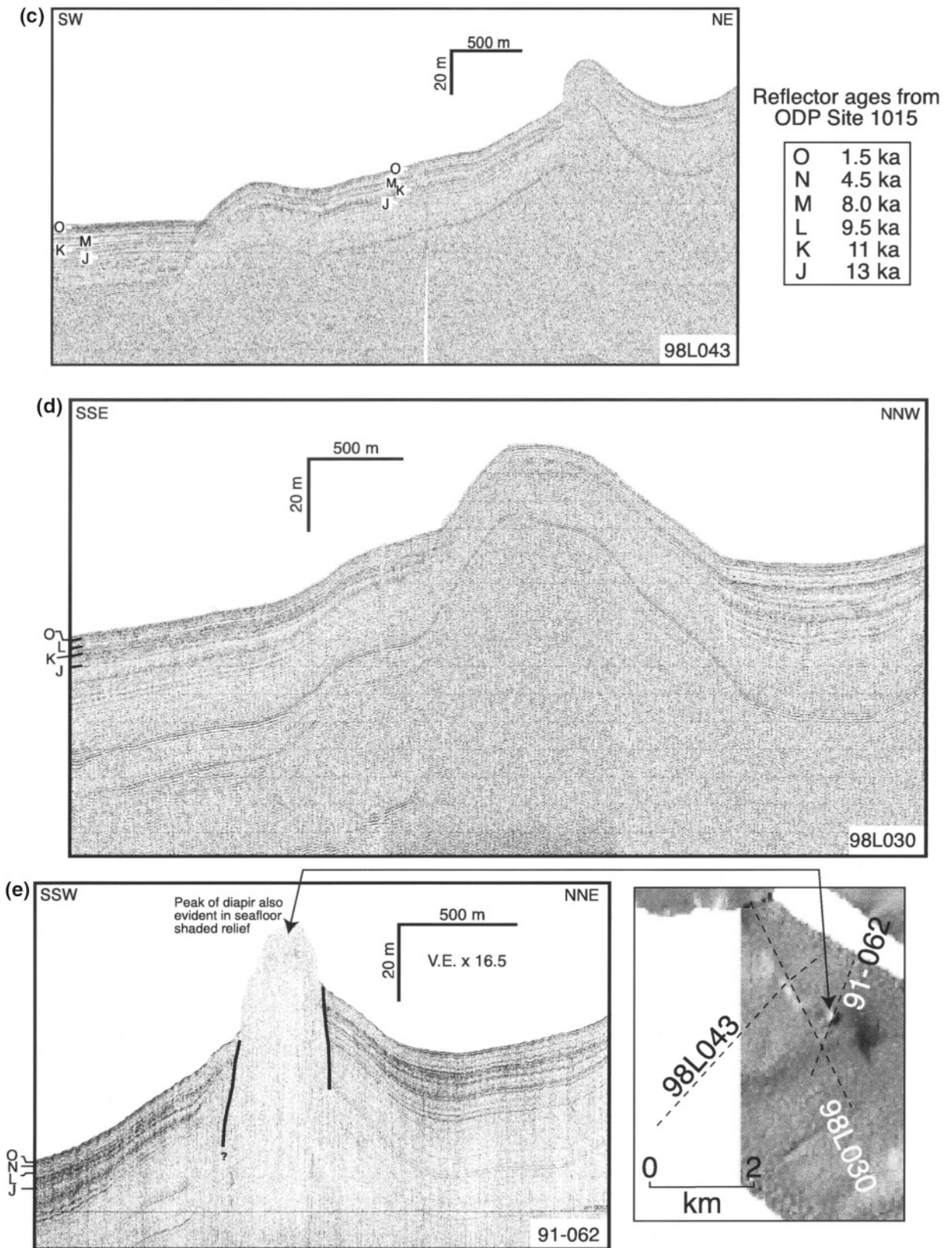


Figure 16. (Continued)

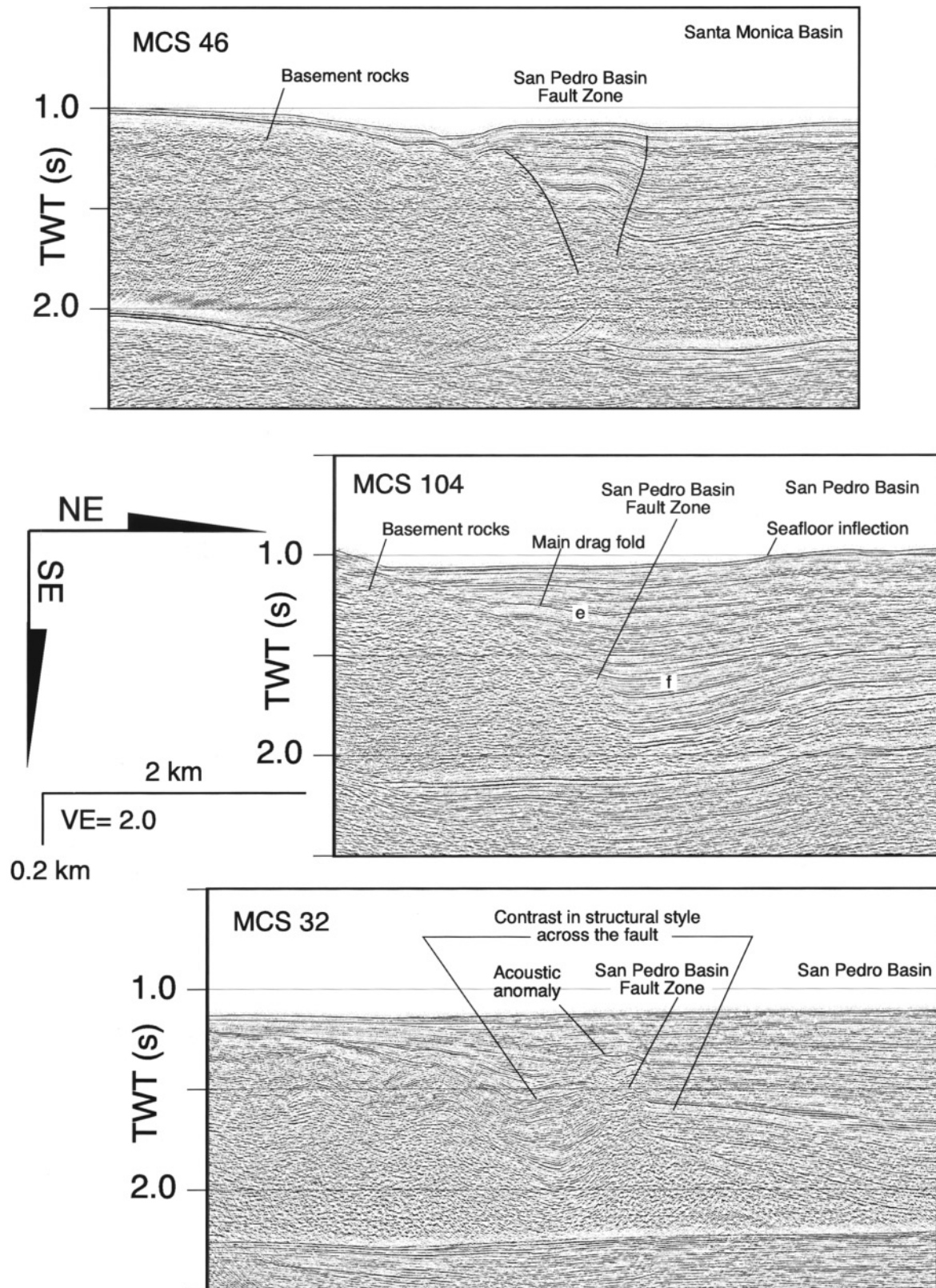


Figure 17. Three poststack-migrated MCS sections across the San Pedro Basin fault zone, showing normal and reverse apparent offset along this strike-slip fault. Figure 4 shows the locations of the sections. An acoustic anomaly developed along the fault zone.

without evident structural interruption near the supposed location of the Palos Verdes Fault.

Despite the difficulty in locating the Palos Verdes Fault using marine seismic-reflection data presented here, some previous reports (e.g., Yerkes *et al.*, 1965; Wright 1992) indicate that this fault extends several tens of kilometers northwest of the peninsula beneath the shelf. This fault is interpreted to have a vertical separation on crystalline basement that is down to the northeast and amounts to about 1 km, as estimated from inferred depth contours (Yerkes *et al.*, 1965). Evidence for this deep fault derives from depths below the level of penetration of our seismic-reflection data. On the basis of data presented here, we interpret that no strand of the Palos Verdes Fault offsets Holocene sediment north of the Palos Verdes Peninsula.

Regional structural and tectonic models may provide clues to how the Palos Verdes Fault should appear in seismic-reflection data; however, significant interpretive difficulty arises from the uncertainty about whether the predominant style of movement along the Palos Verdes Fault is reverse or strike slip. One model that purports to show the structural underpinnings of the area east of Santa Monica Bay (Shaw and Suppe, 1996) indicates that the Palos Verdes Fault splays upward from the blind Compton thrust fault, which is proposed to offset rocks at considerable depth (5–10 km). The Compton thrust fault deforms rocks to a lesser degree in the northwest, the part of the fault Shaw and Suppe (1996) called the Baldwin Hills segment (Figs. 3 and 18), than in the main part of the thrust ramp, which lies to the southeast across a segment boundary. One possibility, then, is that diminished movement to the northwest along the Compton thrust fault may be expressed at shallow depth by the Palos Verdes Fault as it dies out to the northwest beneath Santa Monica Bay.

In another view of the Palos Verdes Fault (Shaw, 1999), it may be a reverse fault that has an apparent southwestern dip and transects much of the upper crust, down to depths as great as 10 km. Hypocenters about 10 km deep, all of which show reverse fault movement, as well as oil-industry seismic reflection data obtained about 10 km southeast of the Palos Verdes Peninsula are interpreted to indicate that for depths shallower than 5 km, the Palos Verdes Fault is vertical or dips steeply west (Shaw, 1999). The hypocenters showing reverse movement are interpreted to mean that between 5 and 10 km, this fault has an apparent southwestern dip at 30°. Ambiguity in this interpretation stems from the distribution of hypocenters, which are aligned almost vertically and not along the indicated fault plane.

If under Santa Monica Bay the Palos Verdes Fault dips west, as proposed in Shaw (1999) for the area southeast of the Palos Verdes Peninsula, then this fault's tip, the eastern limit of its upper plate, could outcrop along the curving course of the Santa Monica Canyon. This possibility is supported by three observations. First, the canyon forms the north and northwest limit of the topographically high-standing part of the shelf (Fig. 10), which may have been uplifted along the supposed, west-dipping reverse fault. A

closely related point is that the canyon lies along the northwest limit of the short-wavelength folding of shelf rocks within the shelf projection anticlinorium. In contrast, across the canyon to the north of the anticlinorium, a weakly deformed sediment wedge underlies the upper slope. Second, north of this canyon metamorphic basement lies mainly deeper than about 2 km, whereas south of the canyon, basement is at shallow depth, less than about 1 km. Third, where the Santa Monica Canyon crosses the San Pedro Escarpment, the escarpment ends abruptly and a low-relief continental slope extends farther north and northwest. This crossing of canyon and escarpment coincides with a significant change in the structure of the San Pedro Basin fault zone. In our view, these differences across the Santa Monica Canyon indicate the presence of a fault, which might be the Palos Verdes Fault.

In contrast to tectonic models that highlight supposed reverse movement along the Palos Verdes Fault, other regional models indicate mainly strike-slip offset along this fault (Nardin and Henyey, 1978; Wright, 1991; McNeilan *et al.*, 1996; Francis *et al.*, 1996; Legg *et al.*, 2001). Evidence in support of the idea that the Palos Verdes Fault and some other offshore faults are strike slip includes that (1) flower structures are evident along some fault segments, as shown by seismic-reflection data presented here (e.g., Fig. 14) and elsewhere (Francis *et al.*, 1996); (2) fault traces are straight, even where they cross significant seafloor relief; (3) the offshore faults parallel the northwest strike of other strike-slip faults associated with the Peninsular Ranges; and (4) secondary structures occur at fault bends, including pull-apart basins and pop-up structures, that are common along strike-slip faults.

The types of structures that develop where strike-slip faults bend are indicated by analog sandbox experiments (McClay and Bonora, 2001), which may be a guide to the types of structures that underlie the study area. Analog models indicate that structures below Santa Monica Bay might include a complex network of folds and faults that are transverse to the main strike-slip fault as well as shallow, high-angle reverse faults that terminate downward at nearly horizontal detachments. Compressively deformed zones where strike-slip faults bend are bounded laterally by subsidiary faults that show combined reverse and strike-slip offset and connect downward with the main strike-slip faults.

These analog models can be used as a guide to the complex rock structure that underlies the Palos Verdes Hills and the shelf projection anticlinorium. That these rocks are deformed by dextral shear, where strike-slip faults bend or end, is explained elsewhere (Narding and Henyey, 1978; Francis *et al.*, 1996; Legg *et al.*, 2001). If the Palos Verdes Fault is strike slip and ends to the northwest under Santa Monica Bay, then the fault may terminate within a complex convergence zone because its motion must be transferred to other faults or otherwise be accommodated within deforming crustal rocks. For example, Legg *et al.* (2001) proposed that the Palos Verdes Fault terminates below Santa Monica Bay,

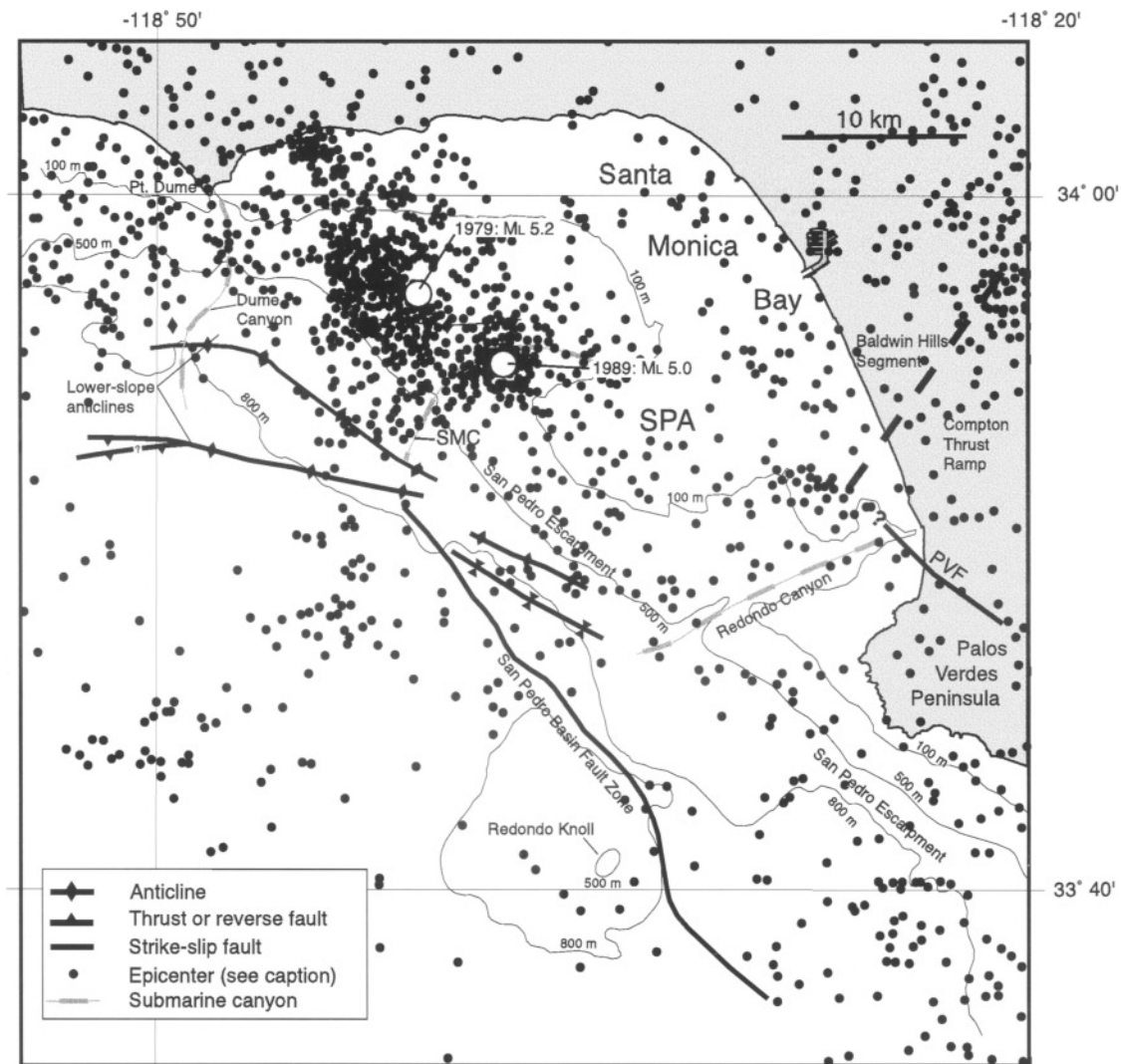


Figure 18. Summary structural findings from this report and earthquake epicenters (from Goter, 1992). The heavy dashed line that extends southwestward just north of the Palos Verdes Peninsula marks the approximate boundary between the Compton thrust ramp and the Baldwin Hills thrust-fault segment (Shaw and Suppe, 1996). PVF, Palos Verdes Fault; SMC, Santa Monica Canyon; SPA, shelf projection anticlinorium.

possibly causing the short-wavelength folding within the shelf projection anticlinorium.

A successful tectonic model for the study area needs to reconcile the observed hypocenters, 5–10 km deep, nearly all of which reveal thrust or reverse movement, with seismic-reflection data that reveal shallow (less than 2 km) rocks deformed by strike-slip and reverse faults. A two-level model that incorporates both observations might involve deep movement along low-angle detachments and reverse faults and an upper-crustal level, similarly deformed, but with the added complication of strike-slip faults. The observed scarcity of hypocenters showing strike-slip movement could mean that these faults are aseismic or that they do not extend downward to the seismogenic zone.

Other faults in the study area that might cause earth-

quakes include the San Pedro Basin fault zone and the fault zone that underlies the San Pedro Escarpment. Both of these fault zones strike northwest, like the Palos Verdes Fault and other faults associated with the Peninsular Ranges. The San Pedro Basin fault zone dips steeply and is probably strike slip, as indicated by the flower structures developed along it. Southeast of the Palos Verdes Peninsula, this fault coincides with the western limit of a dense distribution of small-to moderate-magnitude (M_w 3–5) earthquakes (Bohannon and Geist, 1998). Where this fault and the San Pedro Escarpment converge near the mouth of Santa Monica Canyon, the escarpment ends abruptly and a low-relief continental slope extends farther north and northwest. The lower-slope anticlines that deform rock below this slope show that the fault continues northwest nearly to intersect with the Dume Fault.

Folds and faults under the San Pedro Escarpment extend northwest as far as Santa Monica Canyon. If, as outlined earlier, a major fault, such as the Palos Verdes Fault, follows this canyon and dips west, then the deformation under the escarpment might not extend to great depth but be confined to the upper plate of this fault, in accord with inferences drawn from analog models.

The Dume Fault is related to the east–west Transverse Ranges but is not well imaged in our data because only a few seismic-reflection lines cross the fault and they do so obliquely. Even so, evidence in our seismic-reflection data for Quaternary and probably Holocene activity along this fault includes folding of shallow sediment and arching of the seafloor. The Dume Fault falls within the zone of north–south compression that is thought to have caused the two Malibu earthquakes (Hauksson and Salvidar, 1986, 1989), indicating a high potential for earthquakes along the Dume and parallel faults.

Conclusions

A variety of seismic-reflection data collected in and near Santa Monica Bay have been interpreted to describe the structure and stratigraphy of rocks under the continental shelf and of rocks within the Santa Monica and San Pedro Basins, to the west. This study's main conclusions are as follows.

1. Some offshore faults have moved recently, as indicated by seafloor offset or disruption of very shallow sediment. The Dume Fault, part of the west-striking fault system related to development of the western Transverse Ranges, deforms shallow sediment and arches the seafloor. Locally along the length of the San Pedro Basin fault, the seafloor is offset, but for much of the fault's extent, deformed rocks are buried beneath undeformed sediment. Folds and faults near Redondo Canyon warp or offset the seafloor, but we cannot determine whether the Redondo Canyon Fault itself has been active.
2. The San Pedro Basin Fault is an excellent example of a transpressional, strike-slip fault. It deforms a broad zone within the San Pedro Basin and the adjacent escarpment, as shown by a complicated assemblage of structures arrayed along the fault's length. The geologic structure associated with this fault varies over such short distances that even with seismic-reflection lines spaced apart by about 2 km, individual structural elements within the transpressional zone cannot be correlated along strike.
3. Fill in the San Pedro and Santa Monica Basins may be no older than about 600 ka. This interpretation is based on the two critical assumptions, namely that the rate of sediment deposition has been more or less constant and that sediment compaction can be neglected. The implied, high rates of deposition could have obscured Holocene movement along faults that exhibit no offset of the seafloor or shallow sediment.

4. The part of the Palos Verdes Fault that produces surface breaks apparently dies out northwest of the Palos Verdes Peninsula. Along the projected strike of this fault, no offset is evident either of the seafloor or in shallow sediment under the continental shelf. Other workers (e.g., Yerkes *et al.*, 1965; Wright, 1991), however, show fault offset at depth that extends northwestward beneath the shelf.
5. To aid the assessment of earthquake hazards, sediment cores should be obtained to date the unconformity that spans the location of the Palos Verdes Fault but is not offset (section 101, Fig. 11a). Sediment above this unconformity likely postdates the last sea level rise, which began at about 12 ka ago.
6. An important structural node is the intersection of the Santa Monica Canyon with the San Pedro Escarpment, which extends southeastward from the canyon. The relatively simple structure of two lower-slope anticlines and their associated faulting gives way southeastward across the canyon to a complicated array of faults showing normal and reverse separation.
7. Local features in seismic-reflection data point to the possibility that high pore-fluid pressure accompanied deformation of basin fill. The origin of these fluids is probably within the rapidly deposited, Quaternary sediment, but a fluid source deeper in the crust cannot be discounted.

Acknowledgments

The authors thank Christopher Sorlien and Mark Legg for critical reviews that greatly improved this report.

References

- Aldridge, D. F., and D. W. Oldenburg (1993). Two-dimensional tomographic inversion with finite-difference traveltimes, *J. Seismic Expl.* **2**, 257–274.
- Atwater, T. M. (1970). Implications of plate tectonics for the Cenozoic evolution of western North America, *Geol. Soc. Am. Bull.* **81**, 3513–3536.
- Atwater, T. (1998). Plate tectonic history of the Transverse Ranges and Channel Islands, Southern California, *Am. Assoc. Petrol. Geol. Bull.* **82**, 841.
- Barron, J. A., and C. M. Isaacs (2001). Updated chronostratigraphic framework for the California Miocene, in *The Monterey Formation from Rocks to Molecules*, C. M. Isaacs and J. Rullkotter (Editors), Columbia Univ. Press, New York, 393–395.
- Bohannon, R. G., and E. L. Geist (1998). Upper crustal structure and Neogene tectonic development of the California Continental Borderland, *Geol. Soc. Am. Bull.* **110**, 779–800.
- Bohannon, R. G., S. L. Eittreim, and J. R. Childs (1990). Cruise Report of R/V *S.P. Lee*, Leg 4, 1990, California continental borderland, *U.S. Geol. Surv. Open-File Rept.* 90-0502, 10 pp.
- Brocher, T. M., R. W. Clayton, K. D. Klitgord, R. G. Bohannon, R. Sliter, J. K. McRaney, J. V. Gardner, and J. B. Keene (1995). Multichannel seismic-reflection profiling on the R/V *Maurice Ewing* during the Los Angeles Region Seismic Experiment (LARSE), California, *U.S. Geol. Surv. Open-File Rept.* 95-228.
- Childs, J. R., W. R. Normark, and M. A. Fisher (1999). Permit application and approval chronology for a small airgun survey offshore southern California, June 1999, *U.S. Geol. Surv. Open-File Rept.* 99-572

- (<http://geopubs.wr.usgs.gov/open-file/of99-572/>, last accessed August 2003).
- Clarke, S. H., H. G. Greene, M. E. Field, and W. H. K. Lee (1983). Reconnaissance geology and geologic hazards of selected areas of the southern California borderland, *U.S. Geol. Surv. Open-File Rept.* 83-62, 78 pp.
- Clarke, S. H., H. G. Greene, and M. P. Kennedy (1985). Identifying potentially active faults and unstable slopes offshore, in *Evaluating Earthquake Hazards in the Los Angeles Region: An Earth-Science Perspective*, J. I. Ziony (Editor), *U.S. Geol. Surv. Prof. Pap.* 1360, 347-373.
- Crouch, J. K., and J. Suppe (1993). Late Cenozoic tectonic evolution of the Los Angeles basin and inner California borderland: a model for core complex-like crustal extension, *Geol. Soc. Am. Bull.* **103**, 1415-1434.
- Davis, T. L., and J. Namson (1994a). A balanced cross section of the 1994 Northridge earthquake, southern California, *Nature* **372**, 167-169.
- Davis, T. L., and J. Namson (1994b). Structural analysis and seismic potential evaluation of the Santa Monica Mountains anticlinorium and Elysian Park thrust system of the Los Angeles basin and Santa Monica Bay, National Earthquake Hazard Reduction Program Award 1434-93-G-2292.
- Davis, T., and J. Namson (2002). Nine regional cross sections across the Los Angeles Basin, www.davisnamson.com/downloads/index.htm (last accessed August 2003).
- Davis, T. L., J. Namson, and R. F. Yerkes (1989). A cross section of the Los Angeles area: seismically active fold and belt, the 1987 Whittier Narrows earthquake, and earthquake hazard, *J. Geophys. Res.* **94**, 9644-9664.
- Dolan, J. F., K. Sieh, T. K. Rockwell, R. S. Yeats, and J. Shaw (1995). Prospects for larger, more frequent earthquakes in greater metropolitan Los Angeles, California, *Science* **267**, 199-205.
- Dolan, J. F., K. Sieh, and T. K. Rockwell (2000). Late Quaternary activity and seismic potential of the Santa Monica fault system, Los Angeles, California, *Geol. Soc. Am. Bull.* **112**, 1559-1581.
- Fischer, P. J., R. H. Patterson, C. Darrow, J. H. Rudat, and G. Simila (1987). The Palos Verdes fault zone: onshore to offshore, in *Geology of the Palos Verdes Peninsula and San Pedro Bay*, P. J. Fischer (Editor) Book 55, Pacific Section of the Society of Economic Paleontologists and Mineralogists, Tulsa, Oklahoma, 91-134.
- Francis, R. D., M. R. Legg, D. R. Sigurdson, and P. J. Fischer, (1996). Restraining bend along the Palos Verdes Fault zone, offshore Southern California, *EOS* **77**, no. 46 (Suppl.), 512.
- Fuis, G. S., T. Ryberg, N. J. Godfrey, D. A. Okaya, and J. M. Murphy (2001). Crustal structure and tectonics from the Los Angeles basin to the Mojave Desert, southern California, *Geology* **29**, 15-18.
- Gardner, J. V., and P. Peter Dartnell (2002). Multibeam mapping of the Los Angeles, California margin, *U.S. Geol. Surv. Open-File Rept.* 02-162.
- Goter, S. K. (1992). Southern California earthquakes, *U.S. Geol. Surv. Open-File Rept.* 92-553, scale 1:375,000.
- Greene, H. G., and M. P. Kennedy (Editors) (1987). Geology of the inner southern California continental margin, California Division of Mines and Geology, California Continental margin Geologic Map Series, scale 1:250,000.
- Gutmacher, C. E., W. R. Normark, S. L. Ross, B. D. Edwards, R. Sliter, P. Hart, B. Cooper, J. Childs, and J. A. Reid (2000). Cruise report for A1-00-SC Southern California earthquake hazards project, Part A, *U.S. Geol. Surv. Open-File Rept.* 00-516, 67 pp. (<http://geopubs.wr.usgs.gov/open-file/of00-516/of00-516p.pdf>, last accessed August 2003).
- Hauksson, E., and G. V. Saldívar (1989). Seismicity and active compressional tectonics in Santa Monica Bay, Southern California, *J. Geophys. Res.* **94**, 9591-9606.
- Hauksson, E., and G. V. Saldívar (1986). The 1930 Santa Monica and the 1979 Malibu, California, earthquakes, *Bull. Seism. Soc. Am.* **76**, 1542-1559.
- Hornafius, J. S., B. P. Luyendyk, R. R. Terres, and M. J. Kammerling (1986). Timing and extent of Neogene tectonic rotation in the western Transverse Ranges, California, *Geol. Soc. Am. Bull.* **97**, 1476-1487.
- Jennings, C. W. (1994). An explanatory text to accompany the fault activity map of California and adjacent areas, California Division of Mines and Geology Geologic Data Map 6, 92 pp.
- Junger, A., and H. C. Wagner (1977). Geology of the Santa Monica and San Pedro Basins, California Continental Borderland, U.S. Geol. Surv. Map MF-820, scale 1:250,000.
- Kammerling, M. J., and B. P. Luyendyk (1979). A model for Neogene tectonics of the inner southern California borderland constrained by paleomagnetic data (abstracts with programs), *Geol. Soc. Am.* **11**, 453.
- Legg, M. R. (Compiler) (1987). Earthquake epicenters and selected fault plane solutions of the inner-Southern California continental margin, in *Regional Geologic Map Series*, vol. 1B, H. G. Greene and M. P. Kennedy (Editors), California Division of Mines and Geology.
- Legg, M. R., M. J. Kammerling, and R. Francis (2001). Termination of strike-slip faults at convergence zones within continental transform boundaries: examples from the California Continental Borderland, *EOS* **82**, no. 47, (Fall Meeting Suppl.), F1110.
- Luyendyk, B. P., M. J. Kammerling, and R. R. Terres (1980). Geometric model for Neogene crustal rotations in southern California, *Geol. Soc. Am. Bull.* **91**, I211-I217.
- Luyendyk, B. P., M. J. Kammerling, R. R. Terres, and J. S. Hornafius (1985). Simple shear of southern California during the Neogene, *J. Geophys. Res.* **90**, 12,454-12,466.
- Marlow, M. S., J. V. Gardner, and W. R. Normark (2000). Using high-resolution multibeam bathymetry to identify seafloor surface rupture along the Palos Verdes fault complex in offshore southern California, *Geology* **28**, 587-590.
- McClay, K., and M. Bonora (2001). Analog models of restraining stopovers in strike-slip fault systems, *Am. Assoc. Petrol. Geol.* **85**, 233-260.
- McNeilan, T. W., T. K. Rockwell, and G. Resnik (1996). Style and rate of Holocene slip, Palos Verdes Fault zone, southern California, *J. Geophys. Res.* **101**, 8317-8334.
- Nardin, T. R., and T. L. Heney (1978). Pliocene-Pleistocene diastrophism of Santa Monica and San Pedro shelves, California continental borderland, *Am. Assoc. Petrol. Geol. Bull.* **62**, 247-272.
- Normark, W. R., R. G. Bohannon, R. Sliter, G. Dunhill, D. W. Scholl, J. Laursen, J. A. Reid, and D. Holton (1999a). Cruise report for A1-98-SC Southern California earthquake hazards project, *U.S. Geol. Surv. Open-File Rept.* 99-152, 60 pp.
- Normark, W. R., D. J. W. Piper, and R. N. Hiscott (1998). Sea level controls on the textural characteristics and depositional architecture of the Hueneme and associated submarine fan systems, Santa Monica Basin, California, *Sedimentology* **45**, 53-70.
- Normark, W. R., J. A. Reid, R. W. Sliter, D. Holton, C. E. Gutmacher, M. A. Fisher, and J. R. Childs (1999b). Cruise Report for 01-99-SC: Southern California Earthquake Hazards Project (geopubs.wr.usgs.gov/open-file/of99-560/, last accessed August 2003).
- Petersen, M. D., and S. G. Wesnousky (1994). Fault slip rates and earthquake histories for active faults in southern California, *Bull. Seism. Soc. Am.* **84**, 1608-1649.
- Piper, D. J. W., and W. R. Normark (2001). Sandy fans: from Amazon to Hueneme and beyond, *Am. Assoc. Petrol. Geol. Bull.* **85**, 1407-1438.
- Piper, D. J. W., R. N. Hiscott, and W. R. Normark (1999). Outcrop-scale acoustic facies analysis and latest Quaternary development of Hueneme and Dume submarine fans, offshore California, *Sedimentology* **46**, 47-78.
- Schneider, C. L., C. Hummon, R. S. Yeats, and G. L. Huftile (1996). Structural evolution of the northern Los Angeles basin, California, based on growth strata, *Tectonics* **15**, 341-355.
- Shaw, J. H. (1999). Annual Report, 1999, to the Southern California Earthquake Center: seismic-reflection transect and geologic cross section across the central Los Angeles basin and San Pedro Bay, www.sceec.org/research/99research/99shaw.pdf (last accessed August 2003).

- Shaw, J. H., and P. M. Shearer (1999). An elusive blind-thrust fault beneath metropolitan Los Angeles, *Science* **283**, 1516–1518.
- Shaw, J. H., and J. Suppe (1996). Earthquake hazards of active blind-thrust faults under the central Los Angeles basin, California, *J. Geophys. Res.* **101**, 8623–8642.
- Shipboard Scientific Party (1997). Site 1015, in Proc. ODP, Init. Repts. 167, M. Lyle, I. Koizumi, C. Richter, et al. (Editors), Ocean Drilling Program, College Station, Texas, 805–832.
- Sorlien, C. C. (1999). Rapid subsidence and south propagation of the active Santa Monica Mountains–Channel Islands thrust, Annual Report Southern California Earthquake Center, 5 pp., www.sceec.org/research/99research/ (last accessed August 2003).
- Stephenson, W. J., T. K. Rockwell, J. K. Odum, K. M. Shedlock, and D. A. Okaya (1995). Seismic reflection and geomorphic characterization of the onshore Palos Verdes fault zone, Los Angeles, *Bull. Seism. Soc. Am.* **85**, 943–950.
- Stuart, C. J. (1979). Middle Miocene paleogeography of coastal southern California and the California borderland: evidence from schist-bearing sedimentary rocks, in *Cenozoic Paleogeography of the Western United States*, J. M. Armentrout, M. R. Cole, and H. TerBest Jr. (Editors), Pacific Coast Paleogeography Symposium, no. 3, Pacific Section, Society of Economic Paleontologists and Mineralogists, Los Angeles, California, 29–44.
- ten Brink, U. S., J. Zhang, T. M. Brocher, D. A. Okaya, K. D. Klitgord, and G. S. Fuis (2000). Geophysical evidence for the evolution of the California inner continental borderland as a metamorphic core complex, *J. Geophys. Res.* **105**, 5835–5857.
- Teng, L. S., and D. S. Gorsline (1989). Late Cenozoic sedimentation in California continental borderland basins as revealed by seismic facies analysis, *Geol. Soc. Am. Bull.* **101**, 27–41.
- Tsutsumi, H., R. S. Yeats, and G. J. Huftile (2001). Late Cenozoic tectonics of the northern Los Angeles fault system, California, *Geol. Soc. Am. Bull.* **113**, 454–468.
- Vedder, J. G. (1987). Regional geology and petroleum potential of the southern California borderland, in *Geology and Resource Potential of the Continental Margin of Western North America and Adjacent Ocean Basins: Beaufort Sea to Baja California*, D. W. Scholl, A. Grantz, and J. G. Vedder (Editors), Circum-Pacific Council for Energy and Mineral Resources Earth Science Series, **6**, 403–448.
- Vedder, J. G. (1990). Maps of California continental borderland showing compositions and ages of bottom samples acquired between 1968 and 1979, U.S. Geol. Surv. Miscellaneous Field Studies Map, MF-2122, scale 1:250,000.
- Walls, C., T. Rockwell, K. Mueller, Y. Bock, S. Williams, K. J. Pfanner, J. Dolan, and P. Fang (1998). Escape tectonics in the Los Angeles metropolitan region and implications for seismic risk, *Nature* **394**, 4485–4495.
- Ward, S. N., and G. Valensise (1994). The Palos Verdes terraces, California: bathtub rings from a buried reverse fault, *J. Geophys. Res.* **99**, 4485–4494.
- Weaver, K. D., and J. F. Dolan (2000). Paleoseismology and geomorphology of the Raymond Fault, Los Angeles County, California, *Bull. Seism. Soc. Am.* **90**, 1409–1429.
- Weigand, P. W., K. L. Savage, B. D. Chinn, and T. Reid (1998). Volcanic rocks on the northern Channel Islands, *Am. Assoc. Petrol. Geol. Bull.* **82**, 861.
- Woodring, W. P., M. N. Bramlette, and W. S. W. Kew (1946). Geology and paleontology of the Palos Verdes Hills, California, *U.S. Geol. Surv. Profess. Pap.* **207**, 145 pp.
- Wright, T. L. (1991). Structural geology and tectonic evolution of the Los Angeles Basin, California, in *Active Margin Basins*, K. T. Biddle (Editor), Amer. Assoc. Petroleum Geol. Memoir **52**, 35–134.
- Yerkes, R. F., T. H. McCulloh, J. E. Schoelhamer, and J. G. Vedder (1965). Geology of the eastern Los Angeles basin, southern California, *U.S. Geol. Surv. Profess. Pap.* **420-A**, 57 pp.
- Ziony, J. I., and L. M. Jones (1989). Map showing late Quaternary faults and 1978–1984 seismicity of the Los Angeles region, California, U.S. Geol. Surv. Misc. Field Studies Map MF-1964, scale 1:250,000.
- U.S. Geological Survey, MS 999
345 Middlefield Rd.
Menlo Park, California 94025
mfisher@usgs.gov
(M.A.F., W.R.N., R.G.B., R.W.S.)
- Simon Fraser University
Burnaby, British Columbia, Canada V5A 1S6
(A.J.C.)